AMERICAN SOCIETY FOR MICROBIOLOGY | Molecular and Cellular Biology®

RESEARCH ARTICLE

Growth-Regulated Hsp70 Phosphorylation Regulates Stress Responses and Prion Maintenance

Chung-Hsuan Kao,[a] Seung W. Ryu,[a] Min J. Kim,[a] Xuemei Wen,[a] Oshadi Wimalarathne,[a] Tanya T. Paull[a]

[a]Department of Molecular Biosciences, The University of Texas at Austin, Austin, Texas, USA

ABSTRACT Maintenance of protein homeostasis in eukaryotes under normal growth and stress conditions requires the functions of Hsp70 chaperones and associated co-chaperones. Here, we investigate an evolutionarily conserved serine phosphorylation that occurs at the site of communication between the nucleotide-binding and substrate-binding domains of Hsp70. Ser151 phosphorylation in yeast Hsp70 (Ssa1) is promoted by cyclin-dependent kinase (Cdk1) during normal growth. Phosphomimetic substitutions at this site (S151D) dramatically downregulate heat shock responses, a result conserved with HSC70 S153 in human cells. Phosphomimetic forms of Ssa1 also fail to relocalize in response to starvation conditions, do not associate *in vivo* with Hsp40 cochaperones Ydj1 and Sis1, and do not catalyze refolding of denatured proteins *in vitro* in cooperation with Ydj1 and Hsp104. Despite these negative effects on HSC70/HSP70 function, the S151D phosphomimetic allele promotes survival of heavy metal exposure and suppresses the Sup35-dependent [*PSI*$^{+}$] prion phenotype, consistent with proposed roles for Ssa1 and Hsp104 in generating self-nucleating seeds of misfolded proteins. Taken together, these results suggest that Cdk1 can downregulate Hsp70 function through phosphorylation of this site, with potential costs to overall chaperone efficiency but also advantages with respect to reduction of metal-induced and prion-dependent protein aggregate production.

KEYWORDS chaperone, heat shock, phosphorylation, protein aggregation, protein homeostasis

Protein homeostasis encompasses a network of processes which maintain the functionality of proteins in the cellular environment (1). Nascent polypeptides fold into stable, tertiary structures during and after translation; however, mammalian protein biosynthesis often leads to incorrectly folded proteins, which can ultimately lead to toxic aggregate formation (2–4). The cellular chaperone network is the primary surveillance system that is essential for maintenance of proteome integrity. While the activities of many members of the chaperone family are well studied, the regulation of these critical enzymes under specific stress conditions is not completely understood.

Hsp70-mediated protein folding requires an ATP/ADP exchange cycle and the assistance of cochaperones (3). Two major classes of cochaperones, Hsp110 (nucleotide exchange factors [NEFs]) and Hsp40 (DNAJ-related proteins), cooperate with Hsp70s and regulate the exchange between ATP-bound and ADP-bound states (5). Hsp70 proteins also work as a hub connecting with other chaperones to facilitate translocation between cellular compartments, regulation of newly synthesized proteins, and sequestration and degradation of protein aggregates (6).

Hsp70 proteins are highly conserved in all species (7). In *Saccharomyces cerevisiae*, there are four functionally and structurally redundant Hsp70 proteins, Ssa1 to Ssa4 (Ssa1-4). While Ssa1 and Ssa2 are constitutively expressed similarly to human HSC70 Ssa3 and Ssa4 are induced by heat shock and other forms of stress similarly to human HSP70 (8). Removal of *SSA1-4* simultaneously is lethal in yeast, but constitutive expres-

Citation Kao C-H, Ryu SW, Kim MJ, Wen X, Wimalarathne O, Paull TT. 2020. Growth-regulated Hsp70 phosphorylation regulates stress responses and prion maintenance. Mol Cell Biol 40:e00628-19. https://doi.org/10.1128/MCB.00628-19.

Address correspondence to Tanya T. Paull, tpaull@utexas.edu.

Received 6 January 2020
Returned for modification 5 February 2020
Accepted 18 March 2020
Accepted manuscript posted online 23 March 2020
Published 28 May 2020

sion of any single gene can rescue this lethality (9, 10). Hsp70 orthologs in eukaryotes are targets of many posttranslational modifications, including numerous phosphorylation events (11). Yeast Ssa1 has two known phosphorylation hot spots, one in the N-terminal nucleotide binding domain (NBD) and the other in the C-terminal substrate binding domain (SBD). Some of these phosphorylation events have been characterized and shown to regulate HSP70/SSA-dependent functions, including heat shock responses, polysome association, protein refolding, and protein disaggregation (12). There have also been numerous other posttranslational modifications observed in HSP70 proteins in eukaryotes (11), but most of these are uncharacterized.

Here, we investigated a conserved phosphorylation site in the ATPase domain of Hsp70 enzymes and found that growth-dependent modification of this site regulates Hsp70 function in budding yeast and in mammalian cells. Yeast Ssa1 protein containing a phosphomimetic version of S151 (S151D) showed reduced association with cochaperone and chaperone partners and lower activity in survival of heat stress and reduction of protein disaggregation *in vivo*. In addition, we found that the status of S151 affects Sup35 prion maintenance as well as survival of heavy metal exposure. Based on this evidence, we propose that Ssa1 S151 phosphorylation may be an important regulatory switch for Hsp70 function in eukaryotes.

RESULTS

Ssa1 S151 phosphorylation occurs under normal growth conditions *in vivo* in budding yeast. Multiple phosphorylated serine/threonine residues have been identified in HSP70 proteins (11, 13, 14); however, the potential functions and regulatory roles of these modifications in Hsp70 are not fully understood. To identify and characterize these sites, we analyzed Ssa1 phosphorylation in budding yeast and HSC70 phosphorylation in human cells by quantitative mass spectrometry. In our analysis of posttranslational modifications, we detected and confirmed Ssa1 and HSC70 phosphorylation at S151 and S153 in yeast and humans, respectively, among other modifications (see Table S1 in the supplemental material). The S151 residue is highly conserved among several Hsp70 family members in *S. cerevisiae* and higher eukaryotes (Fig. 1A). The four abundant cytosolic Hsp70 proteins (Ssa1-4) and yeast mitochondrial Hsp70 proteins (Ssc1 and Ssq1) all have a serine at amino acid 151 in the nucleotide-binding domain (NBD), whereas most bacterial and archaeabacterial HSP70 proteins have an alanine at this position.

In Hsp70 proteins, the substrate-binding domain (SBD) docks with the NBD in the ATP-bound state, where the complex has low affinity for its clients (3, 15). With ATP hydrolysis, the SBD is released from this conformation while connected to the NBD via a flexible linker in the ADP-bound state, consistent with predictions of dynamic motion of Hsp70 between different states (16, 17) (Fig. 1B). Interestingly, the A149 residue of DnaK (corresponding to the S151 residue of yeast Ssa1 or the S153 residue of human HSC70/HSP70) is located close to the interface between the NBD and SBD (Fig. S1). We generated a threaded model of yeast Ssa1 using the ATP-bound form of *Escherichia coli* DnaK (PDB ID 4B9Q) (15). This analysis suggests that S151 is likely in close proximity to the SBD in the ATP-bound state (Fig. 1B, inset), although Q442 and K452 in DnaK are not conserved in Ssa1 (N451 and E441, respectively).

S153 in vertebrate Hsc70 orthologs was found to be phosphorylated in a global study of DNA damage-induced phosphorylation (18). In yeast, S151 in SSA1 also resides in an (S/T)Q PIKK motif; however, the role of SSA1 S151 phosphorylation in DNA damage responses is not clear. To investigate this possibility, we generated a custom antibody directed against phospho-S151 and monitored phosphorylation of recombinant green fluorescent protein (GFP)-Flag-Ssa1 expressed in budding yeast and isolated by immunoprecipitation followed by Western blotting of the tagged protein from normally growing cells. The result shows that the antibody recognizes wild-type Ssa1 but not Ssa1 S151A (Fig. 1C), indicating that the antibody is specific for the S151 residue and that the modification occurs under normal growth conditions. We did not observe any increase in phosphorylation with DNA-damaging agents, however (data not

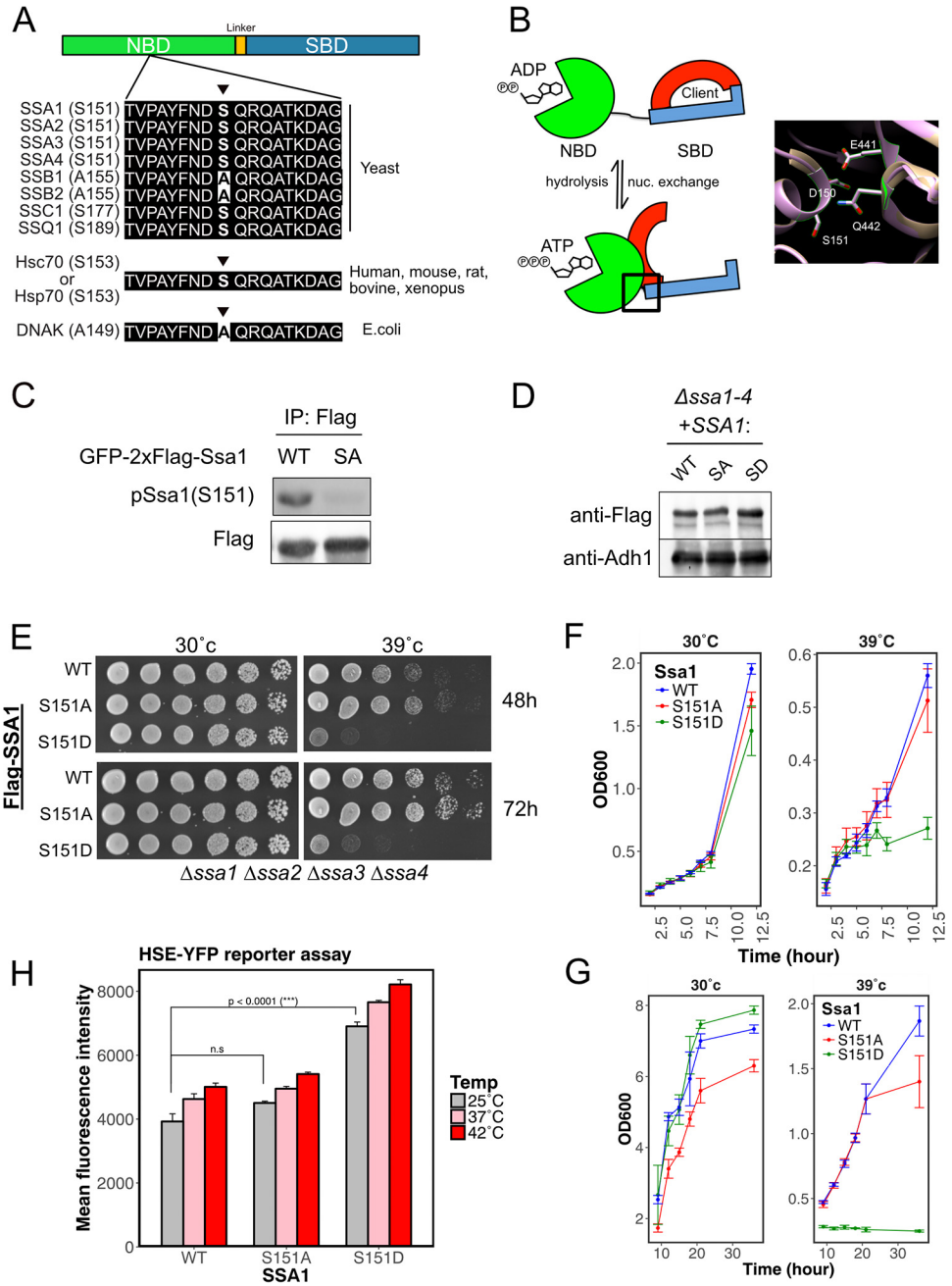

FIG 1 Ssa1 S151 occurs in budding yeast and affects survival of heat shock. (A) Alignment of HSP70 protein sequences in the region surrounding S151 in the NBD in prokaryotic and eukaryotic cells as indicated. (B) The S151 residue of Ssa1 in the NBD is located close to the interaction site with the SBD in the ATP-bound state. (Left panel) ATP hydrolysis and nucleotide exchange are postulated to regulate structural conformation changes in Hsp70 proteins. In the ADP-bound state, the NBD (green) is in an open configuration, connected to the SBD (red, alpha-helical lid; blue, beta-sheet pocket) via a flexible linker. In the ATP-bound state, NBD and SBD undergo a conformational change to interact in a closed configuration. (Right panel) A threaded model of yeast Ssa1 using the crystal structure of the ATP-bound conformation of DnaK (PDB ID 4B9Q) (15). In this model, S151 is in close proximity to the SBD, particularly residues E441 and N451, as shown. See the DnaK structure in Fig. S1 in the supplemental material. (C) GFP-Flag-Ssa1 (wild type [WT]) or GFP-Flag-Ssa1 S151A (S151A) were expressed in a *ssa1 ssa2 ssa3 ssa4* deletion (*Δssa1-4*) strain. GFP-Flag-Ssa1 was isolated by immunoprecipitation and analyzed by quantitative Western blotting with anti-phospho-Hsp70(S151/153) and anti-Flag antibodies. (D) Total lysates from *Δssa1-4* yeast cells expressing Flag-Ssa1 (WT), Flag-Ssa1 S151A (S151A), or Flag-Ssa1 S151D (S151D) were analyzed by Western blotting for Flag or Adh1 as a loading control. (E) *Δssa1-4* yeast cells expressing Flag-Ssa1 (WT), Flag-Ssa1 S151A (S151A), or Flag-Ssa1 S151D (S151D) were spotted in 5-fold serial dilutions and exposed to 30 or 39°C for 48 or 72 h. (F and G) Growth of *Δssa1-4* yeast cells expressing Flag-Ssa1 (WT), Flag-Ssa1 S151A (S151A), or Flag-Ssa1 S151D (S151D) was monitored at 30°C or 39°C as indicated. The growth curve is measured in log phase (F) and stationary phase (G) by OD_{600}. Three

(Continued on next page)

shown). Mass spectrometry analysis of Ssa1 isolated from yeast also showed that the protein is phosphorylated at this site under normal growth conditions (Table S1).

Ssa1 S151 phosphomimetic alleles reduce thermal stability in budding yeast. In order to investigate the role of HSP70 phosphorylation at S151, we expressed Flag-tagged wild-type Ssa1, a nonphosphorylatable mutant Ssa1 (S151A), or a phosphomimetic mutant Ssa1 (S151D) under the control of the Ssa1 natural promoter on a 2μ plasmid in a yeast strain lacking all four Ssa proteins (Fig. 1D) (19). Growth of wild-type and mutant strains was evaluated using a serial spot dilution assay on solid medium (Fig. 1E) or a growth curve in liquid culture (Fig. 1F and G). Both assays indicate that the wild-type and S151A and S151D mutant cells grow similarly at 30°C but that the S151D mutant cells are hypersensitive to high temperature (39°C). Therefore, the phosphomimetic S151D mutant can be considered a temperature-sensitive mutant. Interestingly, we observed that the cells expressing the S151A mutant exhibit a delay in growth as cells approach stationary phase, whereas the cells expressing S151D grow to higher density than the wild type during this period (Fig. 1G).

It is possible that S151D cells exhibit sensitivity to heat shock because of alterations in heat shock factor 1 (Hsf1) regulation (20). In wild-type *S. cerevisiae*, the transcription factor Hsf1 is repressed by Ssa1/2, which binds to Hsf1, preventing its association with heat shock elements (HSEs) (21). Heat shock generates misfolded proteins that compete with Hsf1 for the binding of Ssa1/2, which releases Hsf1 to transcribe HSE-driven genes that generate higher levels of chaperones and repress ribosomal proteins (20, 22, 23). To test for HSF1 activation, we integrated a yellow fluorescence protein (YFP) reporter regulated by HSEs (23) into the genome of our strains and used flow cytometry analysis to monitor HSF1 activity. In the wild-type and S151A strains, exposure to heat (37°C and 42°C) increased the yield of YFP relative to that at 25°C (Fig. 1H) as previously reported (23), although the fold increase with heat is lower in this *ssa1 ssa2 ssa3 ssa4* deletion (Δ*ssa1-4*) strain background than in a wild-type background, likely due to an overall lower level of Hsp70 family members. Cells expressing S151D phosphomimetic Ssa1 exhibited higher HSF1 activation at high temperatures, but this activation was also elevated at 25°C in comparison to that of wild-type and S151A cells. Consistent with this finding of basal derepression of Hsf1, cells expressing S151D Ssa1 under normal growth conditions showed higher levels of expression of several other heat shock proteins and repression of ribosomal proteins (Fig. S2).

HSF1 hyperactivation may be a significant factor in the differential heat sensitivity of cells expressing the S151A and S151D mutants, since deletion of *PIR3*, a proposed target of HSF1 (24, 25), partially rescues the sensitivity of the S151D cells and negates the heat survival advantage of S151A cells (Fig. S3). A similar phenotype was observed with deletion of the phosphatase gene *PPT1*, known to positively regulate HSF1 through dephosphorylation of CK2-modified sites (26, 27).

Ssa1 S151D cells accumulate heat-induced protein aggregates. The impaired heat shock survival of yeast cells expressing Ssa1 S151D protein (Fig. 1D to F) might be related to the accumulation of heat-induced protein aggregates, as Hsp70 proteins have been shown to be critical for dispersal of these toxic products (28). To test this, we collected protein aggregates by separating detergent-insoluble proteins from detergent-soluble proteins by using a previously described method (29). We then compared the overall levels of detergent-insoluble proteins from wild-type and S151A and S151D mutant cells at 30°C or 42°C by Coomassie blue staining of the aggregates on SDS-PAGE gels (Fig. 2A). Interestingly, cells expressing Ssa1 S151D tended to form a higher basal level of total endogenous aggregates

FIG 1 Legend (Continued)
biological replicates were performed, and error bars represent standard deviations. (H) Δ*ssa1-4* yeast cells with an integrated HSE-YFP reporter and expressing Flag-Ssa1 (WT), Flag-Ssa1 S151A (S151A), or Flag-Ssa1 S151D (S151D) were exposed to various temperatures as indicated for 30 min. YFP signal was measured by using a flow cytometer. Three biological replicates were performed with at least 10,000 cells per measurement; error bars represent standard deviations.

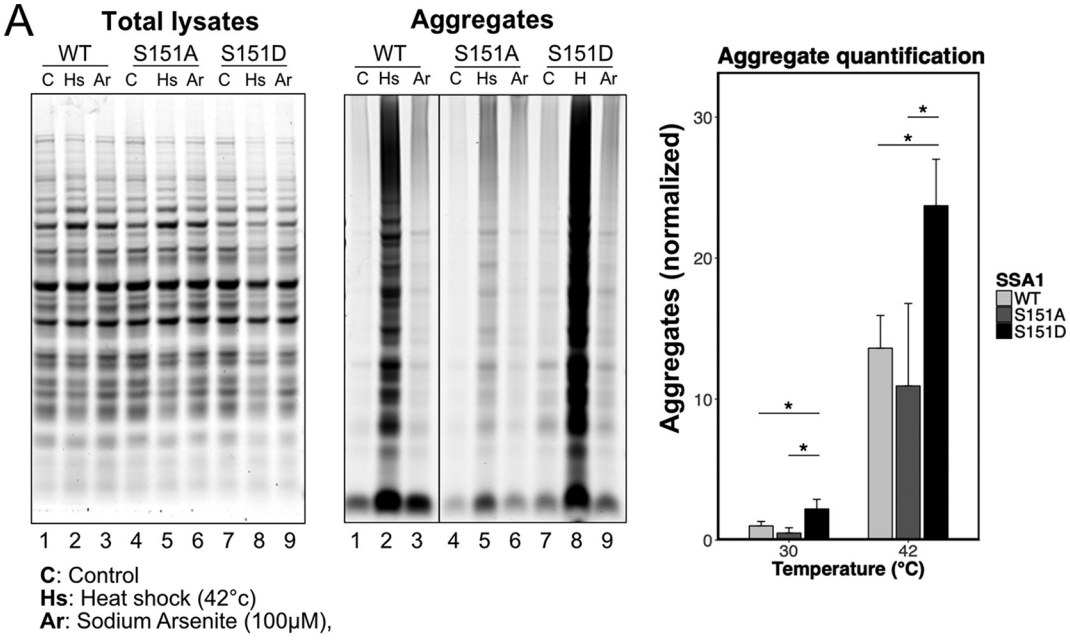

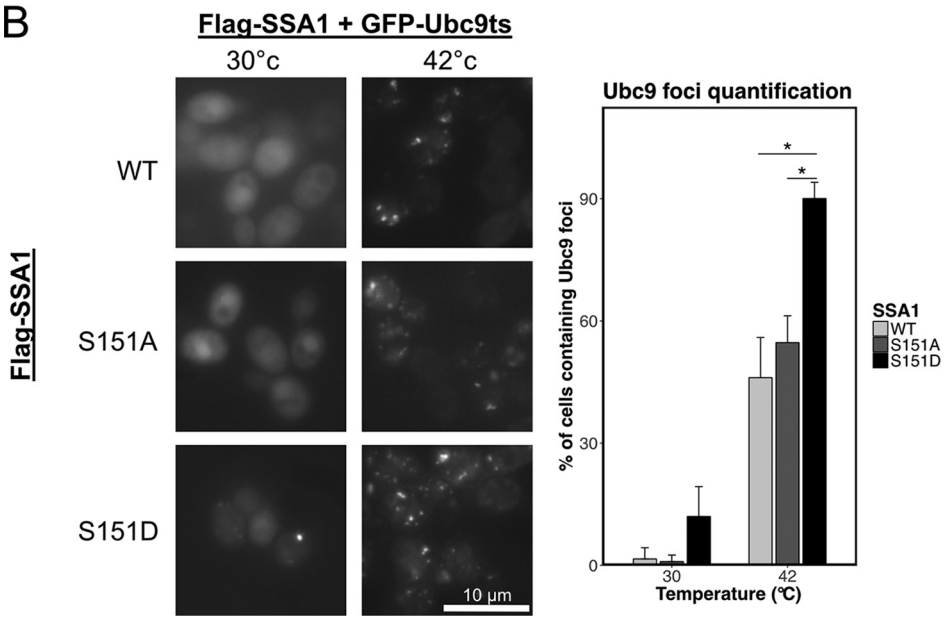

FIG 2 Expression of the Ssa1 S151D phosphomimetic protein promotes heat-induced protein aggregation. (A) (Left and middle panels) Δ*ssa1-4* yeast cells expressing Flag-Ssa1 (WT), Flag-Ssa1 S151A (S151A), or Flag-Ssa1 S151D (S151D) were treated with heat shock (42°C), or sodium arsenite (100 μM) for 60 min. Protein aggregates were isolated (see Materials and Methods) and separated by SDS-PAGE with total lysates. (Right panel) Quantification of the relative amounts of aggregated proteins in each strain (using the total signal per lane), relative to levels of total protein in each lysate (estimated by similar quantitation of lysate, normalized to wild-type Ssa1-expressing cells with no treatment). The *y* axis indicates the quantification measured from the whole lane for aggregate proteins and total proteins. Three biological replicates were performed, and error bars represent standard deviations. *, $P < 0.05$ by Student's two-tailed *t* test. (B) (Left panel) Δ*ssa1-4* yeast cells expressing GFP-Ubc9^{ts} as well as Flag-Ssa1 (WT), Flag-Ssa1 S151A (S151A), or Flag-Ssa1 S151D (S151D) were treated with 30°C or 42°C for 30 min and analyzed by immunofluorescence microscope for Ubc9 foci. (Right panel) Quantification of Ubc9 foci was performed by counting the GFP-positive cells containing at least one GFP focus per cell and dividing that number by the total number of GFP-positive cells. Three biological replicates were performed, and error bars represent standard deviations. *, $P < 0.05$ by Student's two-tailed *t* test.

than wild-type and Ssa1 S151A cells at 30°C (Fig. 2A, lanes C). Similarly, Ssa1 S151D cells produced more heat-induced total aggregates than wild-type and S151A cells at 42°C (Fig. 2A, lanes Hs). The results are consistent with the growth data described above in that S151D cells accumulate more detergent-insoluble proteins than

wild-type and S151A mutant cells during heat exposure. In contrast, the S151A-expressing cells showed lower levels of protein aggregates than wild-type Ssa1-expressing cells, with or without heat treatment, suggesting a higher efficiency of aggregate removal than that of wild-type cells. Arsenite treatment, used here as a general form of oxidative stress, yielded similar levels of aggregates in all strains.

We also used the well-established aggregate reporter Ubc9 Y68L, a temperature-sensitive allele of the SUMO-conjugating enzyme Ubc9 (Ubc9^{ts}), to measure protein aggregates *in vivo* (30, 31). Our results showed that cells expressing Ssa1 S151D form more endogenous GFP-Ubc9 aggregates (GFP foci) at 30°C and also show nearly 2-fold higher levels of heat-induced GFP foci than wild-type and S151A mutant cells at 42°C (Fig. 2B). Taken together, these data suggest that Ssa1 S151 phosphorylation affects the cellular responses to heat and protein homeostasis stress.

Ssa1 S151 is phosphorylated by cyclin-dependent kinase Cdk1. Although we initiated our study of S151 modification with the idea that PIKK enzymes might regulate HSP70 function, analysis of S151 phosphorylation in strains deficient in the yeast PIKK enzymes (*mec1 tel1* strains) did not support this hypothesis (data not shown). A recent study of other Ssa1 modifications showed that T36 phosphorylation on Ssa1 by yeast Cdk1 and Pho85 is important for G_1/S cell cycle control and suggested that Ssa1 is physically associated with Cdk1 and Pho85 (32). Considering this precedent, we hypothesized that cyclin-dependent kinase might phosphorylate Ssa1 S151. To determine if Cdk1 catalyzes Ssa1 S151 phosphorylation, we expressed galactose-inducible Cdk1 (Cdc28) in GFP-Flag-SSA1-expressing cells and analyzed the phosphorylation status of S151 in Ssa1 immunoprecipitated with anti-Flag antibody. The result shows that Cdk1 overexpression increases Ssa1 S151 phosphorylation signal 3-fold, in comparison to Ssa1 S151A as a negative control (Fig. 3A).

We also utilized yeast cells expressing Cdk1-as1, an analog-sensitive version of Cdk1 (33), to evaluate Ssa1 S151 phosphorylation. In this strain, Cdk1 activity can be downregulated by the addition of 1-NM-PP1 analogs that uniquely block the analog-sensitive Cdk1. We overexpressed GFP-Flag-Ssa1 in the Cdk1-as1 strain and immunoprecipitated Ssa1 after 1-NM-PP1 {1-(1,1-dimethylethyl)-3-(1-naphthalenylmethyl)-1H-pyrazolo[3,4-d]pyrimidin-4-amine} treatment, finding that Ssa1 phosphorylation at S151 was partially decreased under these conditions (Fig. 3B). Then, to confirm the phosphorylation *in vitro*, we purified galactose-inducible His-hemagglutinin (HA)-tagged Cdk1 enzyme and evaluated its ability to phosphorylate recombinant wild-type Ssa1 purified from *E. coli*. In comparison to the purified Cdk1 from raffinose cultures, immunoprecipitated material from galactose-induced cultures produced 1.5- to 2-fold higher levels of Ssa1 S151 phosphorylation (Fig. 3C). In addition, the S151 site was found in a global survey of Cdk1 targets in yeast (14).

Lastly, we used purified recombinant Cdk1/cyclin B (human) in a kinase assay with purified, recombinant Ssa1 made in bacteria which showed phosphorylation of S151 (Fig. S4). Taken together, these data suggest that Cdk1 phosphorylates Ssa1 at S151 *in vivo*, although we cannot exclude the possibility that other kinases modify the site in addition to Cdk1.

Starvation conditions reduce S151 phosphorylation. The Tor pathway participates in protein homeostasis through the connection between Tor-mediated nutrient signaling and chaperone-mediated stress responses (34). Here, we tested the effects of stationary-phase TORin (a Tor1 and Tor2 inhibitor) (35), as well as rapamycin, and found that all of these treatments substantially reduce Ssa1 phosphorylation at S151 (Fig. 3D and E). These results are consistent with our observation of Cdk1 control of this phosphorylation, since Tor inhibition blocks cell cycle progression and Cdk1 activity is low in stationary phase (36–38). We also tested the growth of wild-type and mutant strains under Tor inhibition conditions using a growth curve in liquid culture (Fig. 3F) or a serial spot dilution assay on solid medium (Fig. 3G). Both assays indicated that S151D mutant cells exhibit delayed growth in a TOR-inhibited environment, particularly in high-density cultures as cells approach stationary phase. Interestingly, S151A cells

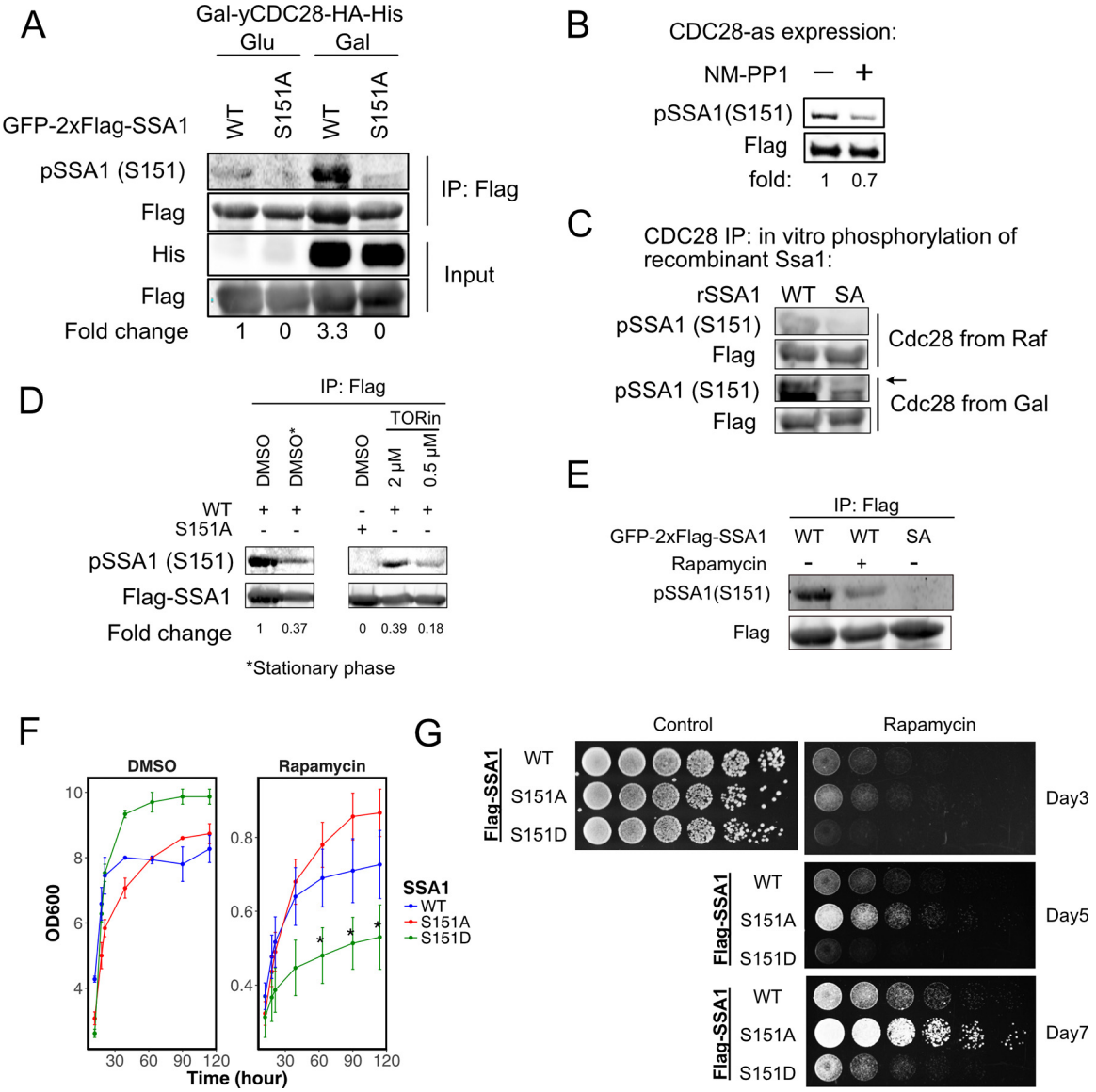

FIG 3 Ssa1 S151 phosphorylation is mediated by Cdk1 and regulated by the TOR pathway. (A) Δ*ssa1-4* yeast cells expressing GFP-Flag-Ssa1 (WT) or GFP-Flag-Ssa1 S151A (S151A) as well as galactose-inducible HA-His-tagged Cdk1 (Gal-yCDC28-HA-His) were grown in glucose (Glu) or galactose (Gal). Ssa1 was isolated by immunoprecipitation and analyzed by Western blotting with anti-phospho-Hsp70(S151/153) (pSSA1), anti-His, and anti-Flag antibodies. (B) Cdk1-as1 cells expressing GFP-Flag-Ssa1 (WT) or GFP-Flag-Ssa1 S151A (S151A) were treated with NM-PP1 (10 μM) for 3 h. Ssa1 was isolated by immunoprecipitation and analyzed by Western blotting with anti-phospho-Ssa1 S151 and anti-Flag antibodies. (C) Recombinant Flag-tagged Ssa1 (WT) or Ssa1 S151A (S151A) was incubated with HA-His-tagged Cdk1 isolated from Δ*ssa1-4* yeast cells expressing galactose-inducible HA-His-tagged Cdk1 (Gal-yCDC28-HA-His) treated with raffinose (Raf) or galactose (Gal). Phosphorylation was analyzed by Western blotting with anti-phospho-Ssa1 S151 and Flag antibodies. An arrow indicates phosphorylated species. (D) Δ*ssa1-4* yeast cells expressing GFP-Flag-Ssa1 (WT) or GFP-Flag-Ssa1 S151A (S151A) were treated with TORin (2 μM or 0.5 μM) for 30 min. Ssa1 was isolated by immunoprecipitation and analyzed by Western blotting with anti-phospho-Ssa1 S151 and anti-Flag antibodies. (E) Δ*ssa1-4* yeast cells expressing GFP-Flag-Ssa1 (WT) or GFP-Flag-Ssa1 S151A (S151A) were treated with rapamycin (200 ng/ml) for 30 min. Ssa1 was isolated by immunoprecipitation and analyzed by quantitative Western blotting with anti-phospho-Ssa1 S151 and anti-Flag antibodies. (F) Δ*ssa1-4* yeast cells expressing Flag-Ssa1 (WT), Flag-Ssa1 S151A (S151A), or Flag-Ssa1 S151D (S151D) were monitored for growth over time in the absence or presence of rapamycin (100 ng/ml). (G) Δ*ssa1-4* yeast cells expressing Flag-Ssa1 (WT), Flag-Ssa1 S151A (S151A), or Flag-Ssa1 S151D (S151D) were spotted in 5-fold serial dilutions on control or rapamycin plates (100 ng/ml), as indicated.

grew to higher densities than wild-type and S151D cells during long-term rapamycin treatment (Fig. 3F and G).

Translation inhibition is a common response to many types of environmental stress (39). Cellular RNA-containing granules form during nutrient deprivation and during stationary phase and serve to protect mRNAs as well as to promote translation

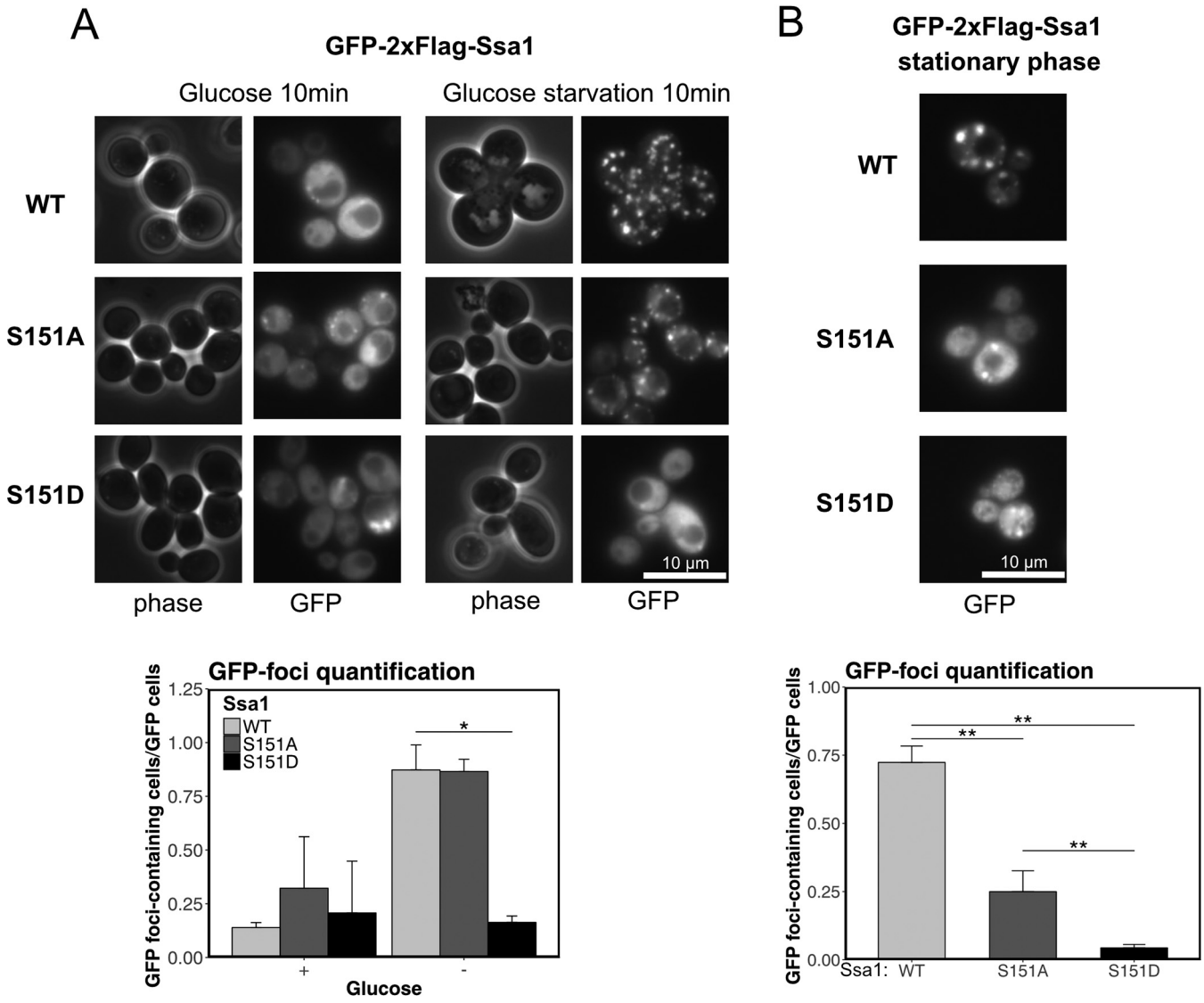

FIG 4 Ssa1 S151 modification affects chaperone localization in response to stress. (A) (Top panel) Δ*ssa1-4* yeast cells expressing GFP-Flag-Ssa1 (WT), GFP-Flag-Ssa1 S151A (S151A), or GFP-Flag-Ssa1 S151D (S151D) were incubated with or without 2% glucose for 10 min and analyzed by fluorescence microscopy. (Bottom panel) Quantification of GFP foci was performed by counting the cells containing at least 1 GFP focus and dividing that number by the total number of GFP-positive cells. Three biological replicates were performed with at least 50 cells counted per measurement; error bars represent standard deviations. *, $P < 0.05$ by Student's two-tailed *t* test. (B) (Top panel) Δ*ssa1-4* yeast cells expressing GFP-Flag-Ssa1 (WT), GFP-Flag-Ssa1 S151A (S151A), or GFP-Flag-Ssa1 S151D (S151D) were incubated at 30°C for 3 days to reach saturation and analyzed by fluorescence microscopy for GFP foci. (Bottom panel) Quantification of GFP foci was performed by counting the cells containing at least 1 GFP focus and dividing that number by the total number of GFP-positive cells. Three biological replicates were performed with at least 50 cells counted per measurement; error bars represent standard deviations. **, $P < 0.05$ by Student's two-tailed *t* test.

reinitiation and elongation after stress conditions are resolved. In budding yeast, Ssa proteins and Hsp40 cochaperones are important for the formation of cytoplasmic ribonucleoprotein (RNP) granules (stress granule and P-bodies) (40). Here, we investigated the efficiency of RNP granule formation by examining GFP-Ssa1 focus formation during glucose deprivation and stationary phase. The results showed that cells expressing Ssa1 S151D completely failed to form RNP granules during glucose deprivation (Fig. 4A). We also examined the behavior of GFP-Ssa1 in stationary phase, during which the chaperone is also known to form discrete foci (41). We observed a lower density of RNP granules in both S151A and S151D mutant cells than in wild-type cells, although S151D expression reduced foci to a greater extent than S151A expression (Fig. 4B). Thus, reorganization of Ssa1 into stress granules is sensitive to the phosphorylation status of S151, with the phosphomimetic allele showing significantly reduced stationary-phase granule formation but the phosphoblocking allele also exhibiting lower efficiency.

S151 modification regulates the interactome of Ssa1. Hsp70 orthologs participate in a wide range of cellular processes through their ATP-dependent cycles of client recognition and protein folding (42). In order to investigate the impact of Ssa1 S151 phosphorylation on the global interactome of Ssa1, we isolated GFP-Flag-tagged Ssa1 wild-type, Ssa1 S151A, and Ssa1 S151D proteins from yeast cells during exponential growth and compared their binding partners by quantitative liquid chromatography-tandem mass spectrometry (LC-MS/MS), using untagged Ssa1 as a negative control for the immunoprecipitation. We detected a total of 2,006 proteins in lysates and immunoprecipitates (Table S2). The bound proteins included known cochaperones and chaperone-associated factors as well as other proteins that may be clients. We identified 46 proteins significantly altered in their binding to S151A-expressing cells in comparison to the wild-type chaperone, while 57 proteins were altered in cells expressing S151D, with three biological replicates from each strain being compared (Fig. 5A to C). These results suggest that Ssa1 S151 status broadly influences the binding between Ssa1 and cellular factors.

J domain-containing proteins (Hsp40s) and nucleotide-exchange factors (NEFs) are the major regulators of Hsp70 in its catalytic cycle (3). Both cochaperones dynamically interact with Hsp70 and carry out diverse functions. Hsp40 proteins transfer substrates to Hsp70 and promote ATP hydrolysis by Hsp70, which transforms Hsp70 into an ADP-bound closed conformation in which the substrate is tightly bound (43). To complete the Hsp70 conformational cycle, NEFs promote the exchange of ADP for ATP and transform Hsp70 back to an ATP-bound open conformation, which releases the folded client (44). Two of the primary Hsp40 enzymes in *S. cerevisiae* are Ydj1 (type I) and Sis1 (type II), each of which independently directs Hsp70 to execute different cellular functions (40, 45, 46). In our coimmunoprecipitation analysis, both Ydj1 and Sis1 were detected with wild-type Ssa1 and the S151A mutant but showed significantly lower association with the Ssa1 phosphomimetic S151D mutant (Fig. 5D and E). In addition, we found that prion-forming factors (Sup35 and Rnq1) exhibited higher association with Ssa1 S151A than with Ssa1 S151D (Fig. 5C; Fig. S5). In contrast, several ribosomal proteins (both small and large subunit) exhibited higher association with Ssa1 S151D than with Ssa1 S151A (Fig. 5C; Table S2).

The binding defect between Ssa1 S151D and the Hsp40 factors may underlie the growth and heat survival deficits observed with this mutant. One possibility we considered was that the S151D mutant phenotype is suppressed by overexpression of the Hsp40 factors that exhibit lower levels of binding. To test this, we overexpressed Ydj1 and Sis1 with an inducible Gal promoter in cells expressing wild-type Ssa1 or Ssa1 S151A or S151D proteins at 30°C (Fig. 5F). Instead of the S151D growth defect being rescued, we found that the S151D-expressing cells were nearly inviable with galactose induction of Ydj1 and Sis1. Thus, the reduction in Ydj1 and Sis1 binding cannot be functionally overcome by overexpression.

In addition to facilitating client binding by Hsp70 proteins, Ydj1 also promotes association between Ssa1 and Hsp104, as well as with small chaperones such as Hsp12, Hsp26, and Hsp31, to promote disaggregation and refolding of aggregated proteins (47–49). Here, we observed that Hsp104 and small chaperones show higher protein expression in cells expressing Ssa1 S151D (Fig. S2), as does Hsp82 (yeast HSP90), which is known to bind directly to Ssa1 (50). Combined with the observation that HSF1 is hyperactive in cells expressing Ssa1 S151D, these observations suggest that Ssa1 phosphorylation may have broad effects on many clients through altered cochaperone binding properties.

Ssa1 S151 status regulates disaggregation by Ssa1, Ydj1, and Hsp104. Previous studies have demonstrated that Ssa1 together with the Hsp40 cochaperone Ydj1 is able to refold misfolded proteins and to prevent the formation of large aggregates from misfolded proteins (2, 51). Budding yeast cells also have the Hsp104 chaperone, which cooperates with Hsp70 and Hsp40 proteins to generate an efficient protein disaggregation assembly (52). Hsp104 is a critical protein disaggregase for yeast cell survival of

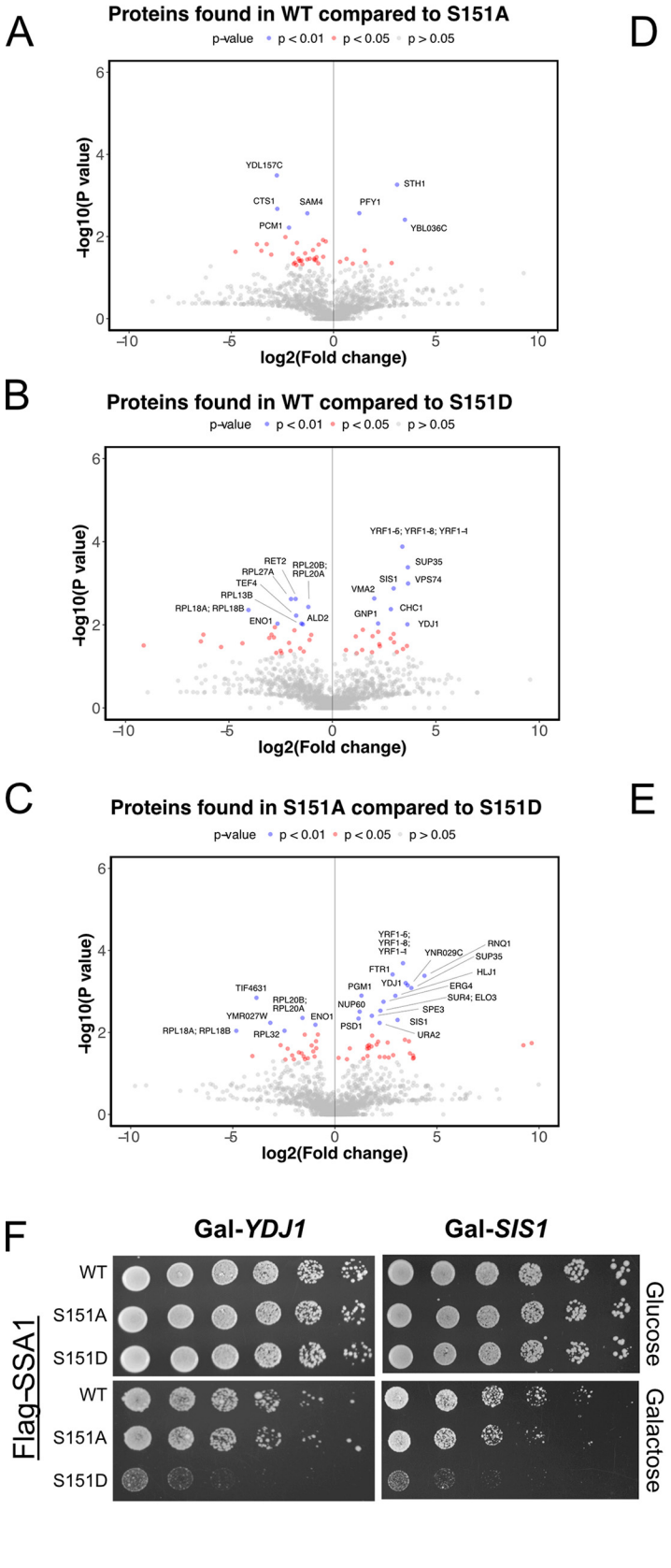

FIG 5 Ssa1 S151 modification affects the interactome of Ssa1. Δ*ssa1-4* yeast cells expressing GFP-Flag-Ssa1 (WT), GFP-Flag-Ssa1 S151A (S151A), or GFP-Flag-Ssa1 S151D (S151D) were grown to exponential phase. Ssa1 was isolated by immunoprecipitation, and binding partners were analyzed by label-free quantitative LC-MS/MS from three biological replicates. (A to C) Volcano plot comparison of Ssa1 binding partners between WT and

(Continued on next page)

severe stress conditions and has been shown to be responsible for extracting polypeptides from protein aggregates in cooperation with Ssa1 and Ydj1 (53).

To directly measure the effects of Ssa1 on protein folding, we established an *in vitro* luciferase-refolding assay with purified recombinant components (Fig. S6). We tested purified wild-type Ssa1, Ssa1 S151A, and Ssa1 S151D proteins *in vitro* with urea-denatured luciferase and found that purified Ssa1 S151D has poor luciferase reactivation efficiency compared to wild-type Ssa1, whereas the S151A mutant is more active than wild-type protein (Fig. 6A). In this case, the Ssa1 proteins were produced in insect cells and the wild-type protein does have S151 phosphorylation (Fig. S6D), so it is expected that the wild type would show an intermediate level of activity compared to the S151A and S151D mutants.

Based on our coimmunoprecipitation observations, Ssa1 S151A and Ssa1 S151D mutants associate with Ydj1 differently, so Ydj1 might play a critical role in controlling refolding or disaggregation functions of Ssa1 in a manner that is controlled by S151 phosphorylation. We found that the combination of purified wild-type Ssa1 and Ydj1 was more efficient in reactivation of urea-denatured luciferase than reaction mixtures containing purified wild-type Ssa1 or purified Ydj1 only (Fig. 6A), consistent with previous reports (52). Both wild-type and S151A proteins were significantly more efficient in luciferase reactivation with Ydj1 present, while the activity of the S151D protein did not improve at all with Ydj1 addition (Fig. 6A), consistent with our binding results in Fig. 5 showing that Ssa1 S151D has reduced binding affinity for Ydj1.

Although Ssa1 and Ydj1 are able to perform a modest level of refolding, previous work has shown that Hsp104 can increase the level of luciferase reactivation by Ssa1 and Ydj1 (52). With purified Ssa1 and Ydj1 in the reaction, we thus compared the efficiency of the reaction with that with recombinant Hsp104 present (Fig. 6B). Consistent with previous results, we also observed that the addition of Hsp104 to wild-type Ssa1 and Ydj1 generated significantly higher levels of reactivated luciferase than reactions without Hsp104 (Fig. 6B). This cooperative effect was also observed with Ssa1 S151A and Ydj1, but Ssa1 S151D and Ydj1 failed to cooperate with Hsp104 in reactivation of aggregated luciferase (Fig. 6B). Without purified Ydj1, we observed that Ssa1 and Hsp104 failed to increase the level of luciferase reactivation although wild-type Ssa1 and Ssa1 S151A still showed more efficient luciferase reactivation than Ssa1 S151D (Fig. 6C). The results indicate that purified Ssa1 S151D fails to form an efficient and functional disaggregase complex with Hsp104 *in vitro*, at least in part due to lack of productive binding to Ydj1. This deficiency is not due to a lack of ATPase activity, as measurements of ATP hydrolysis with purified S151D protein show approximately 2-fold-higher rates of hydrolysis than Ssa1 wild-type or S151A protein *in vitro* (Fig. 6D).

To determine if the effects of Ssa1 S151 phosphorylation are dependent on HSP104-dependent activities *in vivo*, we deleted the *HSP104* gene in our Δ*ssa1-4* yeast strain complemented by wild-type, S151A, or S151D alleles of *SSA1*. The cells were analyzed by serial dilutions on solid medium and also exposed to heat shock at 39°C. The results show that Ssa1 S151D cells exhibit slow growth at elevated temperature compared to wild-type Ssa1-expressing cells while the Ssa1 S151A-expressing cells are even more resistant than wild-type cells (Fig. 6E). Thus, the phosphorylation of S151 (as it occurs in the wild-type strain) yields greater functional deficiencies in the absence of Hsp104 than in its presence.

FIG 5 Legend (Continued)
S151A (A), WT and S151D (B), and S151A and S151D (C), with results of *t* tests summarized by showing $\log_2$ ratios of the fold change between comparisons (*x* axis) and the $-\log_{10}$ of *P* values (*y* axis) for each binding partner identified. Values were normalized by levels of Ssa1 recovered from each immunoprecipitation. Error bars represent standard deviations. *, $P < 0.05$ by Student's two-tailed *t* test. (D) Quantification of Ydj1 binding to WT, S151A, or S151D forms of Ssa1 in immunoprecipitations normalized by total lysates (top panel) compared to the levels in total lysates (bottom panel). (E) Quantification of Sis1 binding to WT, S151A, or S151D forms of Ssa1 in immunoprecipitations normalized by total lysates (top panel) compared to the levels in total lysates (bottom panel). Error bars represent standard deviations. * and **, $P < 0.05$ and $P < 0.01$, respectively, by Student's two-tailed *t* test. (F) Δ*ssa1-4* yeast cells expressing Flag-Ssa1 (WT), Flag-Ssa1 S151A (S151A), or Flag-Ssa1 S151D (S151D) as well as galactose-inducible Ydj1 (Gal-Ydj1) or Sis1 (Gal-Sis1) were spotted on glucose- or galactose-containing plates in 5-fold serial dilutions and grown for 3 days.

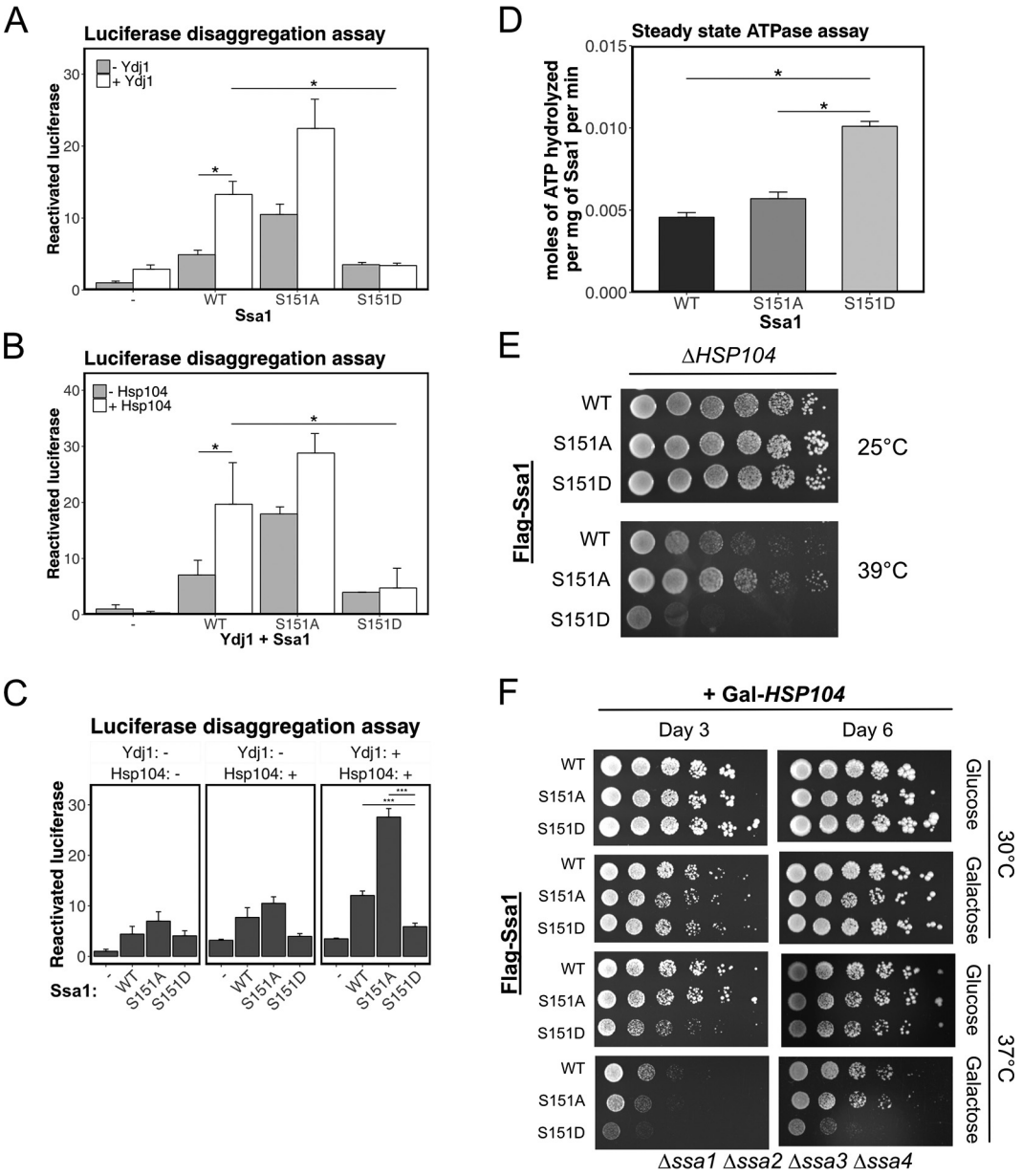

FIG 6 Ssa1 S151 modification affects refolding activity of Ssa1, Ydj1, and Hsp104 *in vitro*. (A) Recombinant wild-type Ssa1, Ssa1 S151A, and Ssa1 S151D proteins (2.5 μM) were incubated with denatured luciferase (3.3×10^4 U) in the presence or absence of Ydj1 (0.4 μM), and steady-state luciferase activity was measured. Three biological replicates were performed, and error bars represent standard deviations. *, $P < 0.05$ by Student's two-tailed *t* test. (B) Recombinant wild-type Ssa1, Ssa1 S151A, Ssa1 S151D, and Ydj1 were tested for luciferase reactivation as described for panel A but also in the presence of Hsp104 (1 μM) as indicated. (C) Comparative summary of luciferase assay results from panels A and B. (D) Steady-state levels of ATP hydrolysis activity of recombinant wild-type Ssa1 (WT), Ssa1 S151A (S151A), and Ssa1 S151D (S151D). Three technical replicates were performed, and error bars represent standard deviations. *, $P < 0.05$ by Student's two-tailed *t* test. (E) Δ*ssa1-4* Δ*Hsp104* yeast cells expressing Flag-Ssa1 (WT), Flag-Ssa1 S151A (S151A), or Flag-Ssa1 S151D (S151D) were spotted in 5-fold serial dilutions and exposed to 30 or 39°C for 120 h. (F) Δ*ssa1-4* yeast cells expressing Flag-Ssa1 (WT), Flag-Ssa1 S151A (S151A), or Flag-Ssa1 S151D (S151D) as well as galactose-inducible Hsp104 (Gal-Hsp104) were spotted in 5-fold serial dilutions and grown on glucose (Glu)- or galactose (Gal)-containing plates, which were incubated at 30°C or 37°C for 3 days or 6 days as indicated.

To test whether additional Hsp104 can recover the heat sensitivity of the S151D mutant strain, we introduced galactose-inducible Hsp104 into the Δ*ssa1-4* strain. Our results showed that additional Hsp104 expression did not affect growth of wild-type, Ssa1 S151A, or Ssa1 S151D cells at 30°C (Fig. 6F). Interestingly, Ssa1 S151D cells with endogenous levels of Hsp104 (glucose) were sensitive to heat shock at 37°C with a short-term incubation (3 days), although they recovered similarly to wild-type cells after

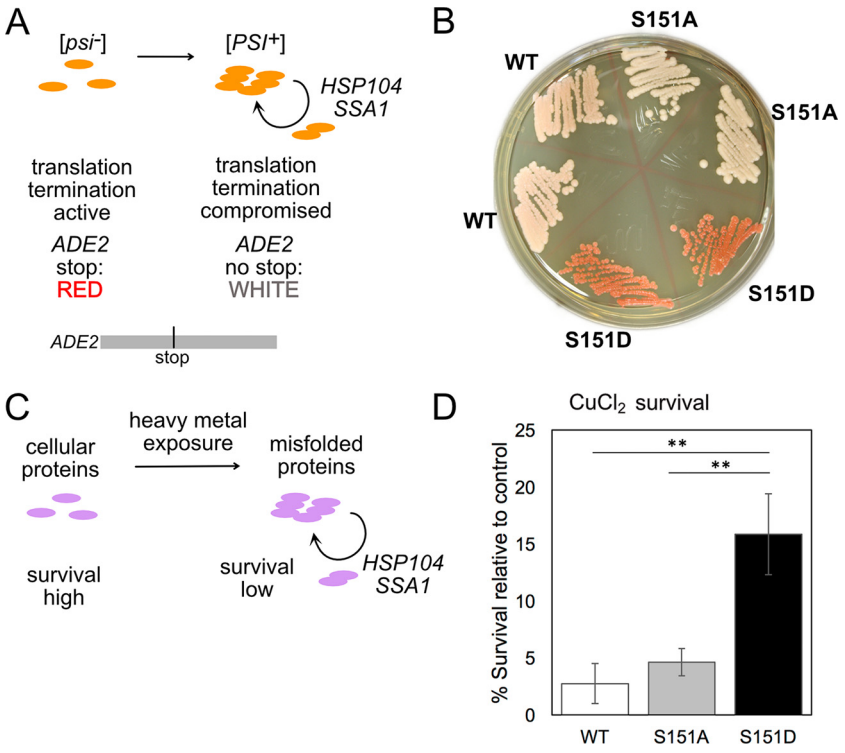

FIG 7 Prion propagation and heavy metal sensitivity are perturbed by Ssa1 S151 modifications. (A) Schematic diagram of [*PSI*$^+$] Sup35 prion formation and propagation through Ssa1/Hsp104-dependent generation of seeds that form new aggregates. Red or white colonies are formed depending on the level of Sup35 function, as indicated. (B) [*PSI*$^+$] Δ*ssa1-4* yeast cells expressing full-length Ssa1 wild type, Ssa1 S151A, or Ssa1 S151D from a CEN plasmid were streaked on YPAD media lacking additional adenine (YPD) plates for 5 days to show the level of *ade2-1* nonsense readthrough. (C) Schematic diagram of heavy metal-induced protein aggregation and propagation through Ssa1/Hsp104-dependent generation of seeds that form new aggregates. (D) Δ*ssa1-4* yeast cells expressing full-length Ssa1 wild type, Ssa1 S151A, or Ssa1 S151D from a CEN plasmid were exposed to $CuCl_2$ (11 mM) for 6 h, followed by washing out of copper and plating on nonselective plates to determine viability. Survival levels relative to that of controls are shown for each strain. **, $P < 0.01$ by *t* test.

a long-term incubation (6 days). However, Ssa1 S151D cells with additional Hsp104 expression in the presence of galactose lost the ability to recover (Fig. 6F). The result indicates that additional Hsp104 might create incomplete or dominant negative disaggregase complexes in the presence of Ssa1 S151D that not only are nonfunctional but also can block protein refolding.

S151 modification impacts Sup35 prion-mediated nonsense suppression. In our coimmunoprecipitation analysis, we observed that Ssa1 is associated with two prion-forming proteins, Rnq1 and Sup35, and that the S151D phosphomimetic form of Ssa1 exhibits significantly lower binding to these proteins (Fig. 5; Fig. S5). The *S. cerevisiae* [*PSI*$^+$] prion is an inheritable, amyloid form of the Sup35 translation termination factor that is deficient in termination function (54). Formation of the amyloid form occurs spontaneously but is promoted by Hsp70 function, specifically Ssa1, as well by the Hsp104 disaggregation machinery, which is required to convert large prion assemblies into smaller units that "seed" new fibers (55–59). Rnq1 has a prion-forming domain that can functionally replace Sup35 and is required for the *de novo* appearance of [*PSI*$^+$] (60, 61). To test whether Ssa1 phosphorylation plays a role in prion propagation, we monitored [*PSI*$^+$] using an Δ*ssa1-4* yeast strain containing an *ade2-1* mutation as a color-based reporter for nonsense codon readthrough (Fig. 7A) (62). In short, [*PSI*$^+$] propagation leads to the generation of functional Ade2 protein (white) due to partial loss of Sup35 termination activity, whereas [*psi*$^-$] cells have normal Sup35 activity and have a red pigment due to lack of Ade2 function. Expression of wild-type, S151A, and S151D versions of *SSA1* in a [*PSI*$^+$] strain showed that [*PSI*$^+$] propagation is maximal

(white colonies) with the S151A mutant, while it is slightly less efficient in wild-type SSA1-expressing cells (slightly pink colonies) after long-term incubation (5 days) (Fig. 7B). In contrast, cells expressing Ssa1 S151D show no apparent [*PSI*$^+$] nonsense suppression (red colonies) (Fig. 7B). These results are consistent with our finding that Ssa1 S151A exhibits higher disaggregation efficiency *in vitro* whereas Ssa1 S151D fails to promote disaggregation under these conditions; however, further investigation is necessary to confirm that this is the case here or whether the readthrough of *ade2-1* is suppressed by Ssa1 S151D in another way.

S151 modification regulates survival of heavy metal exposure. An early report of Δ*hsp104* phenotypes by Sanchez et al. showed that cells lacking this chaperone are dramatically resistant to heavy metal exposure (cadmium and copper) compared to wild-type cells (63), a surprising result considering the general importance of *HSP104* for protein homeostasis in yeast. More recent work suggests that cadmium and copper compounds directly generate misfolding of nascent proteins in budding yeast and higher organisms and that these and other heavy metals generate metal-protein aggregates that seed the formation of new aggregates (64–66). In this sense, metal-induced misfolding intermediates are analogous to prion intermediates in their ability to communicate protein misfolding states (Fig. 7C). To test if Ssa1 S151 phosphorylation may have a similar effect as Δ*hsp104*, we exposed yeast cells expressing wild-type, S151A, or S151D Ssa1 to copper(II) chloride and measured viability. It is clear that the phosphomimetic S151D allele promotes survival of copper exposure under these conditions at a level significantly higher than either S151A or wild-type Ssa1 expression (Fig. 7D), similar to the report for Δ*hsp104* (63). Thus, phosphorylation at S151 is expected to promote heavy metal survival.

S151 modification regulates chaperone function in mammalian cells. As discussed above, Ssa1 S151 is highly conserved in eukaryotes, including humans, where S153 is the corresponding residue in the constitutive HSC70 as well as heat-induced HSP70 (Fig. 1A). HSC70/HSP70 phosphorylation at S153 was observed previously in a study of global SQ/TQ phosphorylation sites in human cells (18), and we found this phosphorylation site in human U2OS osteosarcoma cells as well (Table S1). To confirm that phosphorylation occurs during normal growth, we expressed V5-tagged wild-type HSC70 and a S153A mutant in U2OS cells and isolated the protein by immunoprecipitation, followed by Western blotting with the phosphospecific antibody. The results confirm that S153 phosphorylation does occur in these cells, although residual signal is still present with the S153A mutant, perhaps due to cross-reacting phosphorylation elsewhere in the protein (Fig. 8A).

To investigate the role of HSC70 phosphorylation at S153, we depleted endogenous Hsc70 using small interfering RNA (siRNA); however, in human cells, depletion of HSC70 generates a dramatic induction of HSP70 (HSPA1A/B) expression (Fig. S7) (67). To alleviate this overexpression, we also depleted HSP70, as previously described (67), resulting in 4-fold lower levels of HSC70 with approximately 3-fold-higher levels of Hsp70 relative to untreated cells. In these double-depleted cells, we expressed V5-tagged wild-type HSC70, the nonphosphorylatable mutant HSC70 (S153A), or the phosphomimetic mutant HSC70 (S151D) from a stably integrated doxycycline-inducible promoter (Fig. S7).

We tested for the effect of S153 phosphorylation status on survival of 39°C heat exposure and observed that cells expressing the phosphomimetic S153D mutant were hypersensitive to heat shock (Fig. 8B), consistent with the results we observed in yeast cells (Fig. 1).

HSC70/HSP70 proteins are critical in the nucleolus for ribosome biogenesis, stress responses, and cell signaling (68). In mammalian cells during heat shock, HSC70 rapidly accumulates in nucleoli, a response which is important for counteracting damage and protein misfolding during heat stress (69–71). We tested nucleolus accumulation of GFP-tagged wild-type, S153A, or S153D Hsc70 in U2OS cells during heat shock and found that the Hsc70 S153D phosphomimetic mutant completely failed to accumulate

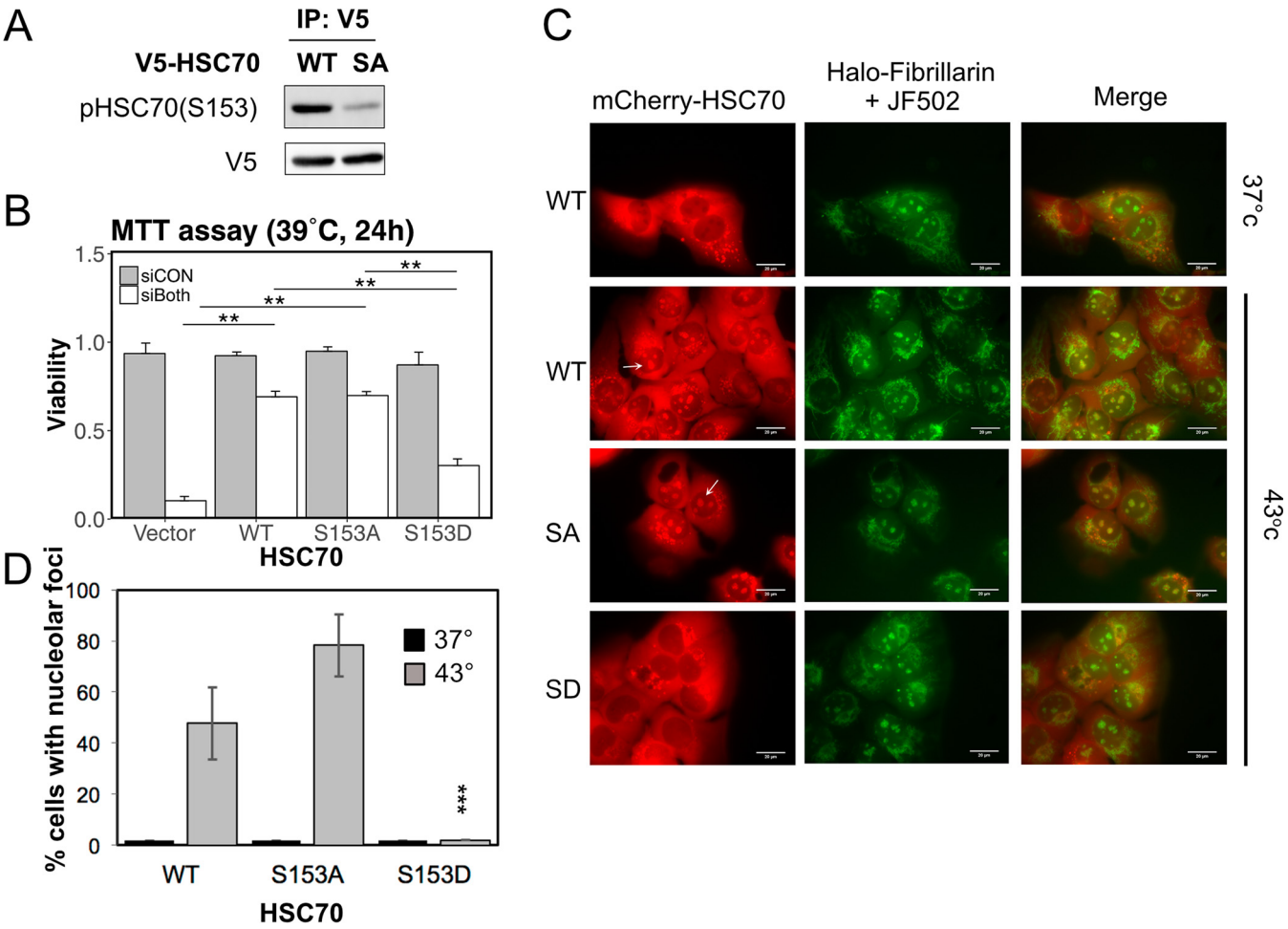

FIG 8 S151 phosphorylation occurs in mammalian cells and regulates heat-induces relocalization of HSC70. (A) V5-Hsc70 (WT) or V5-Hsc70 S153A (SA) were expressed in U2OS cells with concurrent Hsc70/Hsp70 depletion. Hsc70 was isolated by immunoprecipitation and analyzed by Western blotting with anti-phospho-Hsp70(S151/153) and anti-V5 antibodies. (B) U2OS cells expressing V5-Hsc70 (WT), V5-Hsc70 S153A (S153A), or V5-Hsc70 S153D (S153D) were transfected with control siRNA (siCON) or siRNAs directed against HSPA8 (HSC70) and HSPA1A (HSP70) (siBoth) and seeded in 96-wells plates. Cells were treated with doxycycline to induce recombinant Hsc70 expression and incubated at 39°C for 24 h. Cell viability was measured by an MTT [3-(4,5-dimethyl-2-thiazolyl)-2,5-diphenyl-2H-tetrazolium bromide] assay (Thermo Fisher Scientific). Three biological replicates were performed, and error bars represent standard deviations. *, $P < 0.05$ by Student's two-tailed *t* test. (C) mCherry-tagged WT, S153A (SA), or S153D (SD) Hsc70 was expressed in U2OS cells expressing halo-fibrillarin and also treated with the JF502 halotag ligand. Cells were exposed to heat shock (43°C) for 60 min and analyzed by fluorescence microscopy. Arrows indicate nucleolar Hsc70. (D) Quantification of results from panel C showing percentage of cells with overlap between mCherry-Hsc70 and halo-fibrillarin. ***, *P* value of 0.0001 by *t* test for comparison of results for S153D Hsc70 and either wild-type or S153A Hsc70.

in nucleoli compared to wild-type and Hsc70 S153A cells (Fig. 8C and D). Thus, phosphorylation on S153 in Hsc70 is expected to block relocalization in response to heat, similar to the results in budding yeast.

DISCUSSION

Effects of S151 modification on Ssa1 function. The ATPase activity of Hsp70 is dependent mainly on the nucleotide-binding domain (NBD); however, previous studies of bacterial DnaK and DnaJ show that NBD ATPase activity is also tightly coupled to interactions with the substrate-binding domain (SBD) as well as to the binding of cochaperone and peptide clients (72–74). Based on DnaK structures as well as the Hsp70 ortholog Sse1, serine 151 of Ssa1 is predicted to be in a surface-exposed loop of the NBD, juxtaposed against the SBD (Fig. 1B; see Fig. S1 in the supplemental material) (15, 75). Taken together, these data suggest that S151 phosphorylation may play a regulatory role in domain interactions between the NBD and the SBD and also in cochaperone interactions.

Consistent with this prediction, we found that the phosphomimetic version of S151, Ssa1 S151D, exhibits very low levels of binding to Ydj1 and Sis1, cochaperones in the Hsp40 family responsible for escorting clients to Hsp70 and accelerating HSP70 ATP hydrolysis (76–78). Results with recombinant Ssa1 and Ydj1 in an *in vitro* luciferase refolding assay showed that nonphosphorylated Ssa1 (the S151A phosphoblocking mutant) exhibits even higher refolding efficiency than the wild-type Ssa1 protein and that addition of Ydj1 cooperatively increases this activity, as reported previously for Ssa1/Ydj1 (52). In contrast, the S151D mutant failed to promote any cochaperone-mediated refolding, and expression of the Ssa1 S151D phosphomimetic allele *in vivo* results in accumulation of higher levels of more protein aggregates *in vivo* (Fig. 2).

The Hsp104 chaperone is an important disaggregase in budding yeast, functioning cooperatively with Hsp70 and Hsp40 proteins to recognize aggregated proteins and extract individual polypeptides (52, 53). Here, we found that the S151D phosphomimetic Ssa1 failed to cooperate with Hsp104 in luciferase refolding assays *in vitro* and also exhibited more severe heat shock sensitivity in a Δ*hsp104* background *in vivo*. Under these conditions, the S151A form of Ssa1 was remarkably more efficient than wild-type Ssa1 in promoting heat shock survival, suggesting that the unphosphorylated form of Ssa1 can partially compensate for chaperone function normally provided by Hsp104. Expressing higher levels of Hsp104, Ydj1, and Sis1 in Ssa1 S151D strains failed to improve heat shock survival; thus, the functional defect with Ssa1 S151D is not simply a lower affinity of Ssa1 for the cochaperones but more likely involves a conformational change that is incompatible with cochaperone function. A similar combination of attributes was reported with Cdk1 phosphorylation of Ssa1 on T36, also in the NBD (32). In this case, the phosphomimetic version of Ssa1 (T36E) exhibited higher levels of nucleotide binding *in vitro*, low survival of heat shock, reduced binding to Ydj1 (although in this case no effect on Sis1 binding), and altered cell cycle progression (32).

Ssa1 S151 phosphorylation occurs under conditions of rapid growth. Although Ssa1 S151 does not conform to the (S/T)-P (phosphorylated serine or threonine) consensus phosphorylation motif that is normally found for Cdk1 substrates, our data from *in vitro* as well as *in vivo* assays indicate that Cdk1 participates in Ssa1 phosphorylation at S151 (Fig. 3). Non-(S/T)-P sites for Cdk kinases have been reported in other biological contexts (79–84). Ssa1 S151 was also identified in a phosphorylation screen for Cdk1 targets, although the extent of cell cycle dependence was not very high compared to other targets, suggesting that there could also be other kinases responsible for this modification (14). We observed a strong reduction in S151 phosphorylation with Tor inhibition and in stationary phase (Fig. 3), suggesting that if there are other kinases involved, they are likely also subject to growth regulation.

Consistent with the idea that S151 is generally unphosphorylated during conditions of growth inhibition, we found that cells expressing Ssa1 S151A exhibit significantly better growth in the presence of the Tor inhibitor rapamycin than cells expressing either wild-type or S151D Ssa1 (Fig. 3). Previous proteomic analysis of yeast cells grown in the presence of rapamycin indicated that cells with activated Hsf1 are hypersensitive to rapamycin (24). Our finding that Ssa1 S151D-expressing cells show high levels of Hsf1 activation (Fig. 1) is consistent with this and suggests that S151 phosphorylation likely reduces survival during nutrient limitation. It should be noted again here that all of the experiments in this study were done in the context of an *ssa1-4* deletion, and the effects may be more subtle with *SSA1* mutations made in an otherwise wild-type background.

Negative functional effects of S151 modification. The S151D phosphomimetic allele of Ssa1, as well as the S153D form of human HSC70, have mostly negative-acting functional effects on survival of stress conditions and growth. The S151A allele, on the other hand, exhibits either similar or higher activity than the wild-type S151 in these assays, with higher activity associated with Tor inhibition or Hsp104 deficiency. Most

prokaryotes have an alanine at this position, so it is puzzling that eukaryotes have stably inherited and maintained a version of the chaperone that can be inactivated by a kinase that is active during normal growth.

One possibility is that the multiplication of Hsp70 orthologs in eukaryotes has selected for a diversification of functions and binding partners (85). In *S. cerevisiae*, the *SSA* subfamily (Ssa1, Ssa2, Ssa3, Ssa4) is important for protein folding, membrane translocation, nuclear import, and transcriptional responses to a variety of stress conditions, while the *SSB* subfamily (Ssb1 and Ssb2) are key components of the ribosome-associated complex (RAC) that assists the *de novo* folding of newly synthesized polypeptides (19, 86–91). Ssb1 and Ssb2 have an alanine at the 151 position, while all four of the Ssa proteins have a serine. It may be that the ability to phosphorylate Ssa proteins, which is predicted to block Ydj1 and Sis1 binding, promotes associations that are beneficial under other environmental conditions.

Prions and metal-induced misfolded proteins as targets of Hsp70 activity. We show in this work that nonsense suppression by the [*PSI*$^+$] prion is affected by the status of S151 in Ssa1. Hsp70 is well known for its role in prion dynamics, as many laboratories have documented the necessity of Hsp70, Hsp40, and Hsp104 protein families for propagation of the amyloid structures that constitute the infectious and heritable species (54, 57, 62, 92). Previous studies of Hsp70 mutants showed that an L483W change in Ssa1 generates higher rates of ATP hydrolysis, reduced cochaperone binding, and reduced protein refolding efficiency than wild-type Ssa1, as well as a dramatically reduced ability of the protein to promote Sup35-dependent prion propagation (55, 93), all very similar to the Ssa1 S151D mutant described here. In addition, J proteins have been shown to be important for stable propagation of [*PSI*$^+$], [*URE3*], [*SWI*$^+$], and [*RNQ*$^+$] due to critical interactions with Hsp70 (94, 95). Our observation that the Ssa1 S151D mutant shows lower binding to Sis1 may also explain the alterations in [*PSI*$^+$] effects that we have observed in this study.

The idea that misfolded proteins can form seeds that spread misfolding to other, nonaggregated protein species is common to both prions and nascent proteins exposed to heavy metals (64–66). In this sense, optimal chaperone function may be nonproductive, as it can generate new seeds from aggregated species and produce misfolded protein complexes at much higher rates than in the absence of chaperones. The higher viability conferred by the phosphomimetic mutant Ssa1 S151D in the presence of copper shown here suggests that there could be selection for phosphorylation due to pervasive heavy metals in the environment (96) that directly induce protein misfolding.

Our finding that Cdk1 is involved in phosphorylation of S151 suggests that the [*PSI*$^+$] prion as well as metal-induced misfolded protein species would tend to be repressed by phosphorylated Ssa1 S151 in actively growing cultures. [*PSI*$^+$] in yeast affects translation readthrough, a phenomenon proposed to increase the diversity of expressed proteins by translation of 3′ untranslated regions (UTRs) and other normally untranslated sequences (92). It is attractive to consider the possibility that serine 151 phosphorylation is a mechanism by which this evolutionary diversification may be controlled, in effect a switch regulating the appearance of novel polypeptides that is dependent on stress conditions and growth rate. The evolutionary maintenance of S151 in eukaryotic Hsp70 orthologs, perhaps driven by metal exposure, may ultimately regulate diversification advantages through prion regulation of gene expression in a fluctuating environment.

MATERIALS AND METHODS

Yeast strains and plasmids. Yeast strains and plasmids used in this study are listed in Table S3 in the supplemental material. *S. cerevisiae* yeast cultures were grown in synthetic minimal defined medium (0.67% yeast nitrogen base without amino acids, ammonium sulfate, and appropriate amino acids) with 2% glucose or YPAD medium (1% yeast extract, 2% Bacto peptone, 0.004% adenine hemisulfate) with 2% glucose. pESC-URA-GFP-Ubc9ts was a gift from Judith Frydman (Addgene plasmid no. 20369) (30). HSP104-b/Leu(WT) was a gift from Susan Lindquist (Addgene plasmid no. 1156) (97). 5787 pET28aSX104B/pES42 was

a gift from Susan Lindquist (Addgene plasmid no. 1229) (59). pRS315-SSA1 and pDP122 were gifts from Daniel Masison and David Pincus, respectively.

Yeast protein extraction and Western blotting. Yeast cells were grown in 2 ml culture medium for 2 days to stationary phase and inoculated into larger-volume cultures at an optical density at 600 nm (OD_{600}) of 0.15 per ml. Cells were incubated at 30°C until log phase (OD_{600} of 0.3 to 1) and collected at 4,000 rpm for 5 min. Protein was extracted by bead beating in 0.3 ml lysis buffer (25 mM Tris-HCl buffer [pH 7.4], 150 mM NaCl, 1 mM EDTA, 10% glycerol, 0.5% NP-40, 1 mM dithiothreitol [DTT], EDTA-free protease inhibitor [Pierce], and 0.1 ml acid-washed glass beads for 1 min at room temperature. Protein lysates were collected after centrifugation at 3,500 rpm for 5 min at 4°C. Four hundred micrograms of protein lysates was incubated with 50 μl anti-Flag magnetic beads (MBL) for 1 h at 4°C. Beads were collected and washed three times with 500 μl lysis buffer. After the third wash, the lysis buffer was removed completely and the beads were mixed with 20 μl 2.5× SDS sample buffer. The mixture was boiled at 95°C for 5 min. Boiled samples were loaded into 8% SDS-PAGE or NuPAGE 4% to 12% Bis-Tris protein gels (Thermo Fisher). Specific protein targets were analyzed by immunoblot assay with the specific antibodies listed in Table S3. The phospho-Hsp70 (S151/S153) phosphospecific antibody was produced by PhosphoSolutions using a peptide containing the phosphorylated site.

***In vitro* kinase assays.** CDK1 kinase assays were performed in kinase buffer (33 mM Tris-HCl [pH 7.5], 13.3 mM magnesium chloride, 0.5 mM ATP, 5.3 mM DTT) for 60 min at room temperature in a volume of 37.5 μl with 102 nM His-tagged human CDK1-cyclin B (Thermo Fisher Scientific; PV3980) and 370 nM Flag-tagged yeast Ssa1 (wild type and S151A mutant). Phosphorylated Ssa1 S151 was detected using the phosphospecific antibody as described above, with total Ssa1 detected with anti-Flag antibody (Sigma) and Cdk1 detected with an anti-His tag antibody (Rockland).

Galactose induction. Yeast cells were grown in 2 ml culture medium with 2% glucose overnight and then inoculated into 25 ml of synthetic minimal defined medium containing 2% raffinose overnight. This culture was used to inoculate cultures at an OD_{600} of 0.15 with 2% raffinose and incubated at 30°C until log phase (OD_{600} of 0.3 to 1). 3× YP medium (3% yeast extract, 6% peptone, and 6% galactose) was used to induce Gal expression (or glucose-containing medium as a control).

Copper sensitivity. Δ*ssa1-4* yeast cells expressing Ssa1 wild-type, Ssa1 S151A mutant, or Ssa1 S151D mutant proteins were grown to log phase in synthetic minimal defined medium (OD_{600} of ~0.4 to 0.5), 11 mM $CuCl_2$ was added for 6 h, and cells were washed with YPAD medium and plated in dilutions on YPAD plates. Colony survival was measured with three biological replicate experiments comparing cultures with copper exposure to control cultures.

Protein aggregate isolation and analysis. The protein aggregation assay was performed as described previously (29). To prepare cell lysates, the pellets were resuspended in lysis buffer (20 mM Na phosphate [pH 6.8], 10 mM DTT, 1 mM EDTA, 0.1% Tween 20, 1 mM phenylmethylsulfonyl fluoride [PMSF], and EDTA-free protease inhibitor [Pierce]). Cells were lysed in a 4°C water bath-based sonicator (Bioruptor; eight times at level 4.5 and 50% duty cycle) and centrifuged for 20 min at 200 × *g* at 4°C. Supernatants were adjusted to the same concentration, and protein aggregates were pelleted at 16,000 × *g* for 20 min at 4°C. After removal of the supernatants, protein aggregates were washed twice with buffer containing 2% NP-40, 20 mM Na phosphate (pH 6.8), 1 mM PMSF, and EDTA-free protease inhibitor (Pierce), sonicated (six times at level 4.5 and 50% duty cycle), and centrifuged at 16,000 × *g* for 20 min at 4°C. Aggregated proteins were washed in buffer without NP-40 (with sonication four times at level 3 and 50% duty cycle), boiled in 2.5× SDS sample buffer, separated in NuPAGE 4% to 12% Bis-Tris protein gels (Thermo Fisher), and analyzed by Coomassie blue staining. Levels of aggregates were quantified using Image Studio.

Filter-aided sample preparation and trypsin digestion for mass spectrometry. Detergent-resistant aggregates or immunoprecipitated samples were resuspended in 15 μl of 10% SDS sample buffer and 50 mM beta-mercaptoethanol and boiled at 100°C for 5 min. The samples were diluted with 200 μl of UA buffer (8 M urea, 0.1 M Tris-HCl [pH 8.8]) at room temperature. Microcon-30 centrifugal filter units (Millipore; MRCF0R030) were equilibrated with 20% acetonitrile (ACN)–2% formic acid solution (14,000 × *g* for 10 min) prior to use. Diluted samples were loaded on the filters and then washed with UA buffer three times. After washing, samples were reduced with 50 mM DTT in UA buffer, which was added to filters, incubated for 5 min at room temperature, and spun off. The samples were then alkylated with 50 mM iodoacetamide in UA buffer, incubated for 5 min at room temperature, and spun off. Samples were desalted with 40 mM ammonium bicarbonate (ABC) three times. One hundred microliters of 40 mM ABC with 0.5 μl of trypsin gold (Promega; V528A) in phosphate-buffered saline (PBS) was added to samples, and the samples were incubated overnight (37°C). Trypsinized peptides were eluted by centrifugation; filters were washed with 20% ACN–2% formic acid solution, and filtrate was combined with trypsinized peptides eluted in ABC. Peptide samples were dried by lyophilization, desalted with C_{18} tips (Pierce; QK224796) according to the manufacturer's instructions, and resuspended in 80% ACN–2% formic acid for LC-MS/MS analysis at the Proteomics Core Facility (University of Texas at Austin). All centrifugations were done at 14,000 × *g* for 20 min unless otherwise noted. Protein identification by LC-MS/MS was provided by the University of Texas at Austin Proteomics Facility on an Orbitrap Fusion in accordance with previously published procedures (98). Raw files were analyzed using label-free quantification with Proteome Discoverer 2.2 (Thermo Fisher). Any polypeptides with fewer than two unique peptides identified were removed from the final analysis. Refined data were then normalized by the total number of peptide spectrum matches (PSMs) per sample to correct for variation of recovery between samples. Missing data were imputed using weighted low-abundance resampling, which replaces missing values with random values sampled from the lower 5% of the detected values, with heavier weighting toward higher values.

Recombinant protein expression. Wild-type Ssa1, Ssa1 S151A, and Ssa1 S151D proteins were expressed using the Bac-to-Bac baculovirus system (Thermo Fisher). SSA1 wild-type, SSA1 (S151A), and SSA1 (S151D) genes were cloned into pFastBac1 and Flag tagged at the N terminus (generating pTP4416, pTP4417, and pTP4418, respectively). Recombinant bacmid DNA derived from these transfer vectors was transfected into Sf21 insect cells for recombinant baculovirus production according to the manufacturer's instructions. Ssa1 proteins were expressed in Sf21 insect cells after baculovirus infection. Cell pellets were lysed by homogenization and sonicated three times for 40 s in buffer A (25 mM Tris [pH 7.4], 100 mM NaCl, 10% glycerol, 2 mM DTT) containing 0.5% Tween 20, 1 mM PMSF, and 0.001% 2-mercaptoethanol. The lysate was centrifuged for 1 h at 35,000 rpm at 4°C. The supernatant was incubated with ~1 ml M2 anti-Flag antibody-conjugated agarose resin (Sigma) with rotation at 4°C for 1 h. After incubation, the lysate with resin was centrifuged for 3 min at 1,000 × *g*. After removal of the supernatant, the remaining resin was washed with 20 ml of buffer A twice and was eluted with 5 ml of buffer A containing 0.8 mg/ml 3× Flag peptide (Sigma). The buffer with peptide was incubated with the resin for 20 min before elution. The Flag eluate was then loaded onto a 1-ml HiTrap Q column (GE) and washed with buffer A and then eluted with buffer A containing 500 mM NaCl. The eluted protein fractions were dialyzed in buffer A, and the dialyzed fractions were aliquoted frozen in liquid nitrogen and stored at −80°C. Protein concentration was quantified by SDS-PAGE and Coomassie blue staining using a Li-Cor Odyssey imager.

V5-tagged Ydj1 proteins were purified as glutathione *S*-transferase (GST) fusion proteins in *E. coli* BL21. Starter cultures were prepared at 37°C for 16 h. Overnight cultures were diluted 1:20 for an additional 2 h of incubation at 37°C. Isopropyl-β-D-1-thiogalactopyranoside (IPTG) at 100 μM was used to induce protein expression for 3 h at 37°C. Cell pellets were collected at 3,400 rpm for 10 min, resuspended in PBS with 1% Triton, and sonicated for 30 s. Cell supernatants were collected at 10,000 rpm for 10 min and incubated with glutathione-Sepharose 4B resin (GE Healthcare) for 2 h at 4°C. Beads were collected and washed three times with PBS with 1% Triton and three times with 50 mM Tris-HCl (pH 8.0), 150 mM NaCl, 0.01% Triton, and 2.5 mM EDTA. GST fusion protein V5-Ydj1 was subjected to site-specific cleavage with PreScission protease (GE Healthcare) to remove the GST tag. V5-Ydj1 was purified from beads, and its protein concentration was quantified by SDS-PAGE using a Li-Cor Odyssey imager.

Flag-Hsp104 was purified from *E. coli* BL21. Starter cultures were prepared at 37°C for 16 h. Overnight cultures were diluted 1:20 for an additional 2 h of incubation at 37°C. IPTG at 100 μM was used to induce protein expression for 3 h at 37°C. Cell pellets were collected using 3,400 rpm for 10 min. The protein purification protocol step was done as previously described for Ssa1 protein purification.

Luciferase refolding assay. Firefly luciferase (Sigma L9420) was diluted 5-fold with refolding buffer (20 mM Tris-HCl [pH 7.4], 50 mM KCl, 5 mM $MgCl_2$) and denatured with 6 M urea for 30 min at room temperature. Denatured luciferase was then diluted 100-fold with refolding buffer and incubated with the indicated chaperones and cochaperones (see figures and legends), 10 mM ATP, and 10 mM DTT to a final volume of 25 μl. The reaction mixture was incubated at 30°C for 30 min. Five microliters of reaction mixture was mixed with 50 μl luciferase assay substrate (Promega). A Tecan Spark 10M plate reader was used to measure luciferase activity.

ATP hydrolysis measurements. Recombinant proteins were prepared in buffer A (25 mM Tris-HCl [pH 8.0], 100 mM NaCl, 10% glycerol, 1 mM DTT). Reactions were started by adding [α-^{32}P]ATP mixtures (25 mM MOPS [pH 7.0], 5 mM $MgCl_2$, 0.2 mM DTT, 0.1 mg/ml bovine serum albumin [BSA], 50 μM ATP, 50 nM [α-^{32}P]ATP) to protein solutions, followed by incubation at 37°C for 1 h. One microliter of Stop solution (2% SDS and 100 mM EDTA) was added to stop the reaction. One microliter of each reaction mixture was spotted onto a plastic-backed TLC cellulose PEI plate (Scientific Adsorbents, Inc.; no. 78601). The plate was dried and run in 0.75 mM KH_2PO_4 (monobasic) buffer. The percentages of hydrolyzed [α-^{32}P]ATP and [α-^{32}P]ADP were quantified by use of a Typhoon FLA 7000 biomolecular imager and normalized to the reaction without proteins. The normalized percentage of hydrolyzed ATP was divided by the amount of Ssa1 proteins and further divided by the incubation time of the assay.

GFP-Ubc9^{ts} protein aggregate analysis. Galactose-controlled GFP-Ubc9^{ts} was used as an indicator of the level of protein aggregation. Cells were grown overnight and reinoculated into 2 ml of synthetic minimal defined medium with 2% raffinose overnight. Cells were inoculated at 0.15 OD_{600} unit per ml in 2% raffinose and incubated at 30°C until log phase (OD_{600} of 0.3 to 1). Synthetic minimal defined medium with 3× YP medium (2% galactose) was added to induce expression of GFP-Ubc9^{ts} (or 3× YP medium with 2% glucose as a control). Culture medium at 54°C was prepared ahead and used to perform 42°C heat shock at a 1:1 ratio of culture medium. Heated cells were incubated at 42°C for 30 min and then prepared for imaging. Cells with at least one focus were counted as positive and compared to the total number of cells containing GFP fluorescence.

GFP-Ssa1 cellular focus analysis. For the starvation experiment, GPF-tagged Ssa1 wild-type, Ssa1 S151A, and Ssa1 S151D cells were grown overnight and reinoculated into 2 ml of synthetic minimal defined medium with 2% glucose at a concentration of 0.15 OD_{600} unit per ml. Cells were grown to log phase, collected by centrifugation, and then resuspended in medium lacking glucose for 10 min before imaging. Cells with at least one focus were counted as positive and compared to the total number of cells containing GFP fluorescence. For the saturation phase experiment, GPF-tagged Ssa1 wild-type, Ssa1 S151A, and Ssa1 S151D cells were grown for 2 days to saturation phase. Cells with at least one focus were counted as positive and compared to the total number of cells containing GFP fluorescence.

HSE-YFP reporter heat shock assays. The heat shock element (HSE)-YFP reporter, pNH605-4×HSEpr-YFP (pDP122; a gift from David Pincus), was integrated into the genome of the Δ*ssa1-4* yeast cells (a gift from Sabine Rospert). This strain was complemented with Flag-tagged Ssa1 (wild type, S151A

mutant, or S151D mutant). The assay was performed essentially as described previously (23). Briefly, cells were prepared at a density of 0.2 OD_{600} unit per ml and incubated at the indicated temperature (Fig. 1H) on a thermal mixer. After 30 or 60 min, 50 μl was collected and treated with cycloheximide (final concentration, 50 μg/ml) to stop translation. An additional 2 h of incubation at 30°C is required to mature YFP fluorophores. The mean fluorescence intensity (MFI) of each cell was measured using a a BD LSRFortessa flow cytometer and analyzed by FlowJo.

Double siRNA knockdown in human cells. siRNA sequences were designed based on a previous study (67) and are listed in Table S3 in the supplemental material. The transfection of siRNA into U2OS cells was performed with Oligofectamine transfection reagent (Thermo Fisher) according to the manufacturer's instructions. Double knockdowns were performed with a 20 μM concentration of each siRNA.

Heat shock and nucleolin staining of human cells. U2OS cells expressing mCherry-Hsc70 (wild type, S153A mutant, S153D mutant) and halo-fibrillarin were plated into WillCo-dish glass-bottom dishes (catalog no. 14023-200) with cell culture medium containing 1 μg/ml doxycycline one day before the experiment. Cells were heat shocked for 45 min in a 43°C tissue culture incubator (5% CO_2). One picomolar JF502 halotag ligand (a gift from Luke Lavis) was added to the cell medium for 15 min. Finally, cells were washed with sterile PBS at room temperature and then analyzed using a Zeiss Axiovert fluorescent light microscope with a 64× oil immersion objective. Images were analyzed with Fiji software (ImageJ v1.52c). For quantification, at least 70 cells from several fields of view were scored for GFP-HSC70 foci in the nucleolus (overlapping with halo-fibrillarin) under normal growth conditions (37°C) and heat shock (43°C).

Isolation of tagged HSC70 from human cells. Biotinylated, V5-tagged HSC70 was expressed in human U2OS cells and isolated with streptavidin-coated beads under denaturing conditions. Briefly, cells were lysed with urea solution (8 M urea, 50 mM Tris [pH 8], 5 mM $CaCl_2$, 30 mM NaCl, 0.1% SDS, 1:1,000 PMSF/protease inhibitor). Lysates were sonicated for 30 s. Three milligrams of lysates was diluted with 1 M urea. One hundred twenty microliters of streptavidin magnetic beads was added to each sample and rotated overnight at room temperature. The next day, the beads were washed twice for 30 min each with 1 M urea solution (1 M urea, 50 mM Tris [pH 8], 5 mM $CaCl_2$, 30 mM NaCl, 0.1% SDS) at room temperature. The beads were then washed with LiCl (500 mM) for 30 min at room temperature and then washed three times, once each with 0.1% SDS, 0.2% SDS, and 0.5% SDS for 30 min at room temperature. Finally, samples were eluted with 1% SDS with 2-mercaptoethanol at 100°C. Samples were frozen at −20°C until analyzed by filter-assisted sample preparation and trypsinization (see above).

SUPPLEMENTAL MATERIAL

Supplemental material is available online only.

SUPPLEMENTAL FILE 1, PDF file, 1.7 MB.

SUPPLEMENTAL FILE 2, XLSX file, 1.1 MB.

SUPPLEMENTAL FILE 3, XLSX file, 1.5 MB.

SUPPLEMENTAL FILE 4, XLSX file, 0.04 MB.

ACKNOWLEDGMENTS

We are indebted to several individuals at laboratories for yeast strains and reagents, i.e., Sabine Rospert, David Pincus, David Morgan, Daniel Masison, and Luke Lavis, and to Caleb Swaim for help with expression constructs. We also thank Judith Frydman for pESC-URA-GFP-Ubc9ts (Addgene plasmid no. 20369) and Susan Lindquist for HSP104-b/Leu(WT) (Addgene plasmid no. 1156) and pET28aSX104B/pES42 (Addgene plasmid no. 1229). We thank Daniel Masison and members of the Paull laboratory for helpful comments.

C.-H. Kao was supported in part by a Technologies Incubation Scholarship from the Taiwan Ministry of Education.

REFERENCES

1. Kim YE, Hipp MS, Bracher A, Hayer-Hartl M, Hartl FU. 2013. Molecular chaperone functions in protein folding and proteostasis. Annu Rev Biochem 82:323–355. https://doi.org/10.1146/annurev-biochem-060208-092442.
2. Balchin D, Hayer-Hartl M, Hartl FU. 2016. In vivo aspects of protein folding and quality control. Science 353:aac4354. https://doi.org/10.1126/science.aac4354.
3. Saibil H. 2013. Chaperone machines for protein folding, unfolding and disaggregation. Nat Rev Mol Cell Biol 14:630–642. https://doi.org/10.1038/nrm3658.
4. Soto C. 2003. Unfolding the role of protein misfolding in neurodegenerative diseases. Nat Rev Neurosci 4:49–60. https://doi.org/10.1038/nrn1007.
5. Kampinga HH, Craig EA. 2010. The HSP70 chaperone machinery: J proteins as drivers of functional specificity. Nat Rev Mol Cell Biol 11:579–592. https://doi.org/10.1038/nrm2941.
6. Chen B, Retzlaff M, Roos T, Frydman J. 2011. Cellular strategies of protein quality control. Cold Spring Harb Perspect Biol 3:a004374. https://doi.org/10.1101/cshperspect.a004374.
7. Daugaard M, Rohde M, Jäättelä M. 2007. The heat shock protein 70 family: highly homologous proteins with overlapping and distinct functions. FEBS Lett 581:3702–3710. https://doi.org/10.1016/j.febslet.2007.05.039.
8. Verghese J, Abrams J, Wang Y, Morano KA. 2012. Biology of the heat shock response and protein chaperones: budding yeast (Saccharomyces cerevisiae) as a model system. Microbiol Mol Biol Rev 76:115–158. https://doi.org/10.1128/MMBR.05018-11.
9. Werner-Washburne M, Stone DE, Craig EA. 1987. Complex interactions

among members of an essential subfamily of hsp70 genes in Saccharomyces cerevisiae. Mol Cell Biol 7:2568–2577. https://doi.org/10.1128/mcb.7.7.2568.
10. Hasin N, Cusack SA, Ali SS, Fitzpatrick DA, Jones GW. 2014. Global transcript and phenotypic analysis of yeast cells expressing Ssa1, Ssa2, Ssa3 or Ssa4 as sole source of cytosolic Hsp70-Ssa chaperone activity. BMC Genomics 15:194. https://doi.org/10.1186/1471-2164-15-194.
11. Cloutier P, Coulombe B. 2013. Regulation of molecular chaperones through post-translational modifications: decrypting the chaperone code. Biochim Biophys Acta 1829:443–454. https://doi.org/10.1016/j.bbagrm.2013.02.010.
12. Beltrao P, Albanèse V, Kenner LR, Swaney DL, Burlingame A, Villén J, Lim WA, Fraser JS, Frydman J, Krogan NJ. 2012. Systematic functional prioritization of protein posttranslational modifications. Cell 150:413–425. https://doi.org/10.1016/j.cell.2012.05.036.
13. Albuquerque CP, Smolka MB, Payne SH, Bafna V, Eng J, Zhou H. 2008. A multidimensional chromatography technology for in-depth phosphoproteome analysis. Mol Cell Proteomics 7:1389–1396. https://doi.org/10.1074/mcp.M700468-MCP200.
14. Holt LJ, Tuch BB, Villén J, Johnson AD, Gygi SP, Morgan DO. 2009. Global analysis of Cdk1 substrate phosphorylation sites provides insights into evolution. Science 325:1682–1686. https://doi.org/10.1126/science.1172867.
15. Kityk R, Kopp J, Sinning I, Mayer MP. 2012. Structure and dynamics of the ATP-bound open conformation of Hsp70 chaperones. Mol Cell 48:863–874. https://doi.org/10.1016/j.molcel.2012.09.023.
16. Flaherty KM, DeLuca-Flaherty C, McKay DB. 1990. Three-dimensional structure of the ATPase fragment of a 70K heat-shock cognate protein. Nature 346:623–628. https://doi.org/10.1038/346623a0.
17. Zhu X, Zhao X, Burkholder WF, Gragerov A, Ogata CM, Gottesman ME, Hendrickson WA. 1996. Structural analysis of substrate binding by the molecular chaperone DnaK. Science 272:1606–1614. https://doi.org/10.1126/science.272.5268.1606.
18. Matsuoka S, Ballif BA, Smogorzewska A, McDonald ER, Hurov KE, Luo J, Bakalarski CE, Zhao Z, Solimini N, Lerenthal Y, Shiloh Y, Gygi SP, Elledge SJ. 2007. ATM and ATR substrate analysis reveals extensive protein networks responsive to DNA damage. Science 316:1160–1166. https://doi.org/10.1126/science.1140321.
19. Jaiswal H, Conz C, Otto H, Wölfle T, Fitzke E, Mayer MP, Rospert S. 2011. The chaperone network connected to human ribosome-associated complex. Mol Cell Biol 31:1160–1173. https://doi.org/10.1128/MCB.00986-10.
20. Trotter EW, Berenfeld L, Krause SA, Petsko GA, Gray JV. 2001. Protein misfolding and temperature up-shift cause G1 arrest via a common mechanism dependent on heat shock factor in Saccharomyces cerevisiae. Proc Natl Acad Sci U S A 98:7313–7318. https://doi.org/10.1073/pnas.121172998.
21. Sorger PK, Pelham HR. 1988. Yeast heat shock factor is an essential DNA-binding protein that exhibits temperature-dependent phosphorylation. Cell 54:855–864. https://doi.org/10.1016/s0092-8674(88)91219-6.
22. Rowley A, Johnston GC, Butler B, Werner-Washburne M, Singer RA. 1993. Heat shock-mediated cell cycle blockage and G1 cyclin expression in the yeast Saccharomyces cerevisiae. Mol Cell Biol 13:1034–1041. https://doi.org/10.1128/mcb.13.2.1034.
23. Zheng X, Krakowiak J, Patel N, Beyzavi A, Ezike J, Khalil AS, Pincus D. 2016. Dynamic control of Hsf1 during heat shock by a chaperone switch and phosphorylation. Elife 5:e18638. https://doi.org/10.7554/eLife.18638.
24. Bandhakavi S, Xie H, O'Callaghan B, Sakurai H, Kim D-H, Griffin TJ. 2008. Hsf1 activation inhibits rapamycin resistance and TOR signaling in yeast revealed by combined proteomic and genetic analysis. PLoS One 3:e1598. https://doi.org/10.1371/journal.pone.0001598.
25. Hahn J-S, Hu Z, Thiele DJ, Iyer VR. 2004. Genome-wide analysis of the biology of stress responses through heat shock transcription factor. Mol Cell Biol 24:5249–5256. https://doi.org/10.1128/MCB.24.12.5249-5256.2004.
26. Cho B-R, Lee P, Hahn J-S. 2014. CK2-dependent inhibitory phosphorylation is relieved by Ppt1 phosphatase for the ethanol stress-specific activation of Hsf1 in Saccharomyces cerevisiae. Mol Microbiol 93:306–316. https://doi.org/10.1111/mmi.12660.
27. Millson SH, Piper PW. 2014. Insights from yeast into whether the inhibition of heat shock transcription factor (Hsf1) by rapamycin can prevent the Hsf1 activation that results from treatment with an Hsp90 inhibitor. Oncotarget 5:5054–5064. https://doi.org/10.18632/oncotarget.2077.
28. Mogk A, Bukau B, Kampinga HH. 2018. Cellular handling of protein aggregates by disaggregation machines. Mol Cell 69:214–226. https://doi.org/10.1016/j.molcel.2018.01.004.
29. Koplin A, Preissler S, Ilina Y, Koch M, Scior A, Erhardt M, Deuerling E. 2010. A dual function for chaperones SSB-RAC and the NAC nascent polypeptide-associated complex on ribosomes. J Cell Biol 189:57–68. https://doi.org/10.1083/jcb.200910074.
30. Kaganovich D, Kopito R, Frydman J. 2008. Misfolded proteins partition between two distinct quality control compartments. Nature 454:1088–1095. https://doi.org/10.1038/nature07195.
31. Betting J, Seufert W. 1996. A yeast Ubc9 mutant protein with temperature-sensitive in vivo function is subject to conditional proteolysis by a ubiquitin- and proteasome-dependent pathway. J Biol Chem 271:25790–25796. https://doi.org/10.1074/jbc.271.42.25790.
32. Truman AW, Kristjansdottir K, Wolfgeher D, Hasin N, Polier S, Zhang H, Perrett S, Prodromou C, Jones GW, Kron SJ. 2012. CDK-dependent Hsp70 phosphorylation controls G1 cyclin abundance and cell-cycle progression. Cell 151:1308–1318. https://doi.org/10.1016/j.cell.2012.10.051.
33. Bishop AC, Ubersax JA, Petsch DT, Matheos DP, Gray NS, Blethrow J, Shimizu E, Tsien JZ, Schultz PG, Rose MD, Wood JL, Morgan DO, Shokat KM. 2000. A chemical switch for inhibitor-sensitive alleles of any protein kinase. Nature 407:395–401. https://doi.org/10.1038/35030148.
34. Conn CS, Qian S-B. 2011. mTOR signaling in protein homeostasis: less is more? Cell Cycle 10:1940–1947. https://doi.org/10.4161/cc.10.12.15858.
35. Huang H, Chen J, Lu H, Zhou M, Chai Z, Hu Y. 2017. Two mTOR inhibitors, rapamycin and Torin 1, differentially regulate iron-induced generation of mitochondrial ROS. Biometals 30:975–980. https://doi.org/10.1007/s10534-017-0059-1.
36. Barbet NC, Schneider U, Helliwell SB, Stansfield I, Tuite MF, Hall MN. 1996. TOR controls translation initiation and early G1 progression in yeast. Mol Biol Cell 7:25–42. https://doi.org/10.1091/mbc.7.1.25.
37. Hartwell LH, Culotti J, Pringle JR, Reid BJ. 1974. Genetic control of the cell division cycle in yeast. Science 183:46–51. https://doi.org/10.1126/science.183.4120.46.
38. Mendenhall MD, Jones CA, Reed SI. 1987. Dual regulation of the yeast CDC28-p40 protein kinase complex: cell cycle, pheromone, and nutrient limitation effects. Cell 50:927–935. https://doi.org/10.1016/0092-8674(87)90519-8.
39. Cherkasov V, Hofmann S, Druffel-Augustin S, Mogk A, Tyedmers J, Stoecklin G, Bukau B. 2013. Coordination of translational control and protein homeostasis during severe heat stress. Curr Biol 23:2452–2462. https://doi.org/10.1016/j.cub.2013.09.058.
40. Walters RW, Muhlrad D, Garcia J, Parker R. 2015. Differential effects of Ydj1 and Sis1 on Hsp70-mediated clearance of stress granules in Saccharomyces cerevisiae. RNA 21:1660–1671. https://doi.org/10.1261/rna.053116.115.
41. Narayanaswamy R, Levy M, Tsechansky M, Stovall GM, O'Connell JD, Mirrielees J, Ellington AD, Marcotte EM. 2009. Widespread reorganization of metabolic enzymes into reversible assemblies upon nutrient starvation. Proc Natl Acad Sci U S A 106:10147–10152. https://doi.org/10.1073/pnas.0812771106.
42. Clerico EM, Tilitsky JM, Meng W, Gierasch LM. 2015. How hsp70 molecular machines interact with their substrates to mediate diverse physiological functions. J Mol Biol 427:1575–1588. https://doi.org/10.1016/j.jmb.2015.02.004.
43. Mayer MP. 2013. Hsp70 chaperone dynamics and molecular mechanism. Trends Biochem Sci 38:507–514. https://doi.org/10.1016/j.tibs.2013.08.001.
44. Sharma SK, De los Rios P, Christen P, Lustig A, Goloubinoff P. 2010. The kinetic parameters and energy cost of the Hsp70 chaperone as a polypeptide unfoldase. Nat Chem Biol 6:914–920. https://doi.org/10.1038/nchembio.455.
45. Fan C-Y, Lee S, Ren H-Y, Cyr DM. 2004. Exchangeable chaperone modules contribute to specification of type I and type II Hsp40 cellular function. Mol Biol Cell 15:761–773. https://doi.org/10.1091/mbc.e03-03-0146.
46. Rüdiger S, Schneider-Mergener J, Bukau B. 2001. Its substrate specificity characterizes the DnaJ co-chaperone as a scanning factor for the DnaK chaperone. EMBO J 20:1042–1050. https://doi.org/10.1093/emboj/20.5.1042.
47. Fan C-Y, Lee S, Cyr DM. 2003. Mechanisms for regulation of Hsp70 function by Hsp40. Cell Stress Chaperones 8:309–316.
48. Cashikar AG, Duennwald M, Lindquist SL. 2005. A chaperone pathway in protein disaggregation. Hsp26 alters the nature of protein aggregates to facilitate reactivation by Hsp104. J Biol Chem 280:23869–23875. https://doi.org/10.1074/jbc.M502854200.
49. Duennwald ML, Echeverria A, Shorter J. 2012. Small heat shock proteins

potentiate amyloid dissolution by protein disaggregases from yeast and humans. PLoS Biol 10:e1001346. https://doi.org/10.1371/journal.pbio.1001346.
50. Kravats AN, Hoskins JR, Reidy M, Johnson JL, Doyle SM, Genest O, Masison DC, Wickner S. 2018. Functional and physical interaction between yeast Hsp90 and Hsp70. Proc Natl Acad Sci U S A 115:E2210–E2219. https://doi.org/10.1073/pnas.1719969115.
51. Becker J, Walter W, Yan W, Craig EA. 1996. Functional interaction of cytosolic hsp70 and a DnaJ-related protein, Ydj1p, in protein translocation in vivo. Mol Cell Biol 16:4378–4386. https://doi.org/10.1128/mcb.16.8.4378.
52. Glover JR, Lindquist S. 1998. Hsp104, Hsp70, and Hsp40: a novel chaperone system that rescues previously aggregated proteins. Cell 94:73–82. https://doi.org/10.1016/s0092-8674(00)81223-4.
53. Lee J, Kim J-H, Biter AB, Sielaff B, Lee S, Tsai F. 2013. Heat shock protein (Hsp) 70 is an activator of the Hsp104 motor. Proc Natl Acad Sci U S A 110:8513–8518. https://doi.org/10.1073/pnas.1217988110.
54. Liebman SW, Chernoff YO. 2012. Prions in yeast. Genetics 191:1041–1072. https://doi.org/10.1534/genetics.111.137760.
55. Needham PG, Masison DC. 2008. Prion-impairing mutations in Hsp70 chaperone Ssa1: effects on ATPase and chaperone activities. Arch Biochem Biophys 478:167–174. https://doi.org/10.1016/j.abb.2008.07.023.
56. Hung G-C, Masison DC. 2006. N-terminal domain of yeast Hsp104 chaperone is dispensable for thermotolerance and prion propagation but necessary for curing prions by Hsp104 overexpression. Genetics 173:611–620. https://doi.org/10.1534/genetics.106.056820.
57. Chernoff YO, Lindquist SL, Ono B, Inge-Vechtomov SG, Liebman SW. 1995. Role of the chaperone protein Hsp104 in propagation of the yeast prion-like factor [psi+]. Science 268:880–884. https://doi.org/10.1126/science.7754373.
58. Sharma D, Masison DC. 2009. Hsp70 structure, function, regulation and influence on yeast prions. Protein Pept Lett 16:571–581. https://doi.org/10.2174/092986609788490230.
59. Shorter J, Lindquist S. 2004. Hsp104 catalyzes formation and elimination of self-replicating Sup35 prion conformers. Science 304:1793–1797. https://doi.org/10.1126/science.1098007.
60. Sondheimer N, Lindquist S. 2000. Rnq1: an epigenetic modifier of protein function in yeast. Mol Cell 5:163–172. https://doi.org/10.1016/s1097-2765(00)80412-8.
61. Derkatch IL, Bradley ME, Hong JY, Liebman SW. 2001. Prions affect the appearance of other prions. Cell 106:171–182. https://doi.org/10.1016/s0092-8674(01)00427-5.
62. Jung G, Jones G, Wegrzyn RD, Masison DC. 2000. A role for cytosolic hsp70 in yeast [PSI(+)] prion propagation and [PSI(+)] as a cellular stress. Genetics 156:559–570.
63. Sanchez Y, Taulien J, Borkovich KA, Lindquist S. 1992. Hsp104 is required for tolerance to many forms of stress. EMBO J 11:2357–2364. https://doi.org/10.1002/j.1460-2075.1992.tb05295.x.
64. Jacobson T, Priya S, Sharma SK, Andersson S, Jakobsson S, Tanghe R, Ashouri A, Rauch S, Goloubinoff P, Christen P, Tamás MJ. 2017. Cadmium causes misfolding and aggregation of cytosolic proteins in yeast. Mol Cell Biol 37:e00490-16. https://doi.org/10.1128/MCB.00490-16.
65. Tamás M, Sharma S, Ibstedt S, Jacobson T, Christen P. 2014. Heavy metals and metalloids as a cause for protein misfolding and aggregation. Biomolecules 4:252–267. https://doi.org/10.3390/biom4010252.
66. Hane F, Leonenko Z. 2014. Effect of metals on kinetic pathways of amyloid-β aggregation. Biomolecules 4:101–116. https://doi.org/10.3390/biom4010101.
67. Powers MV, Clarke PA, Workman P. 2008. Dual targeting of HSC70 and HSP72 inhibits HSP90 function and induces tumor-specific apoptosis. Cancer Cell 14:250–262. https://doi.org/10.1016/j.ccr.2008.08.002.
68. Bański P, Kodiha M, Stochaj U. 2010. Chaperones and multitasking proteins in the nucleolus: networking together for survival? Trends Biochem Sci 35:361–367. https://doi.org/10.1016/j.tibs.2010.02.010.
69. Kose S, Furuta M, Imamoto N. 2012. Hikeshi, a nuclear import carrier for Hsp70s, protects cells from heat shock-induced nuclear damage. Cell 149:578–589. https://doi.org/10.1016/j.cell.2012.02.058.
70. Frottin F, Schueder F, Tiwary S, Gupta R, Körner R, Schlichthaerle T, Cox J, Jungmann R, Hartl FU, Hipp MS. 2019. The nucleolus functions as a phase-separated protein quality control compartment. Science 365:342–347. https://doi.org/10.1126/science.aaw9157.
71. Nollen EAA, Salomons FA, Brunsting JF, Want J. v d, Sibon OCM, Kampinga HH. 2001. Dynamic changes in the localization of thermally unfolded nuclear proteins associated with chaperone-dependent protection. Proc Natl Acad Sci U S A 98:12038–12043. https://doi.org/10.1073/pnas.201112398.
72. Flynn G, Chappell T, Rothman J. 1989. Peptide binding and release by proteins implicated as catalysts of protein assembly. Science 245:385–390. https://doi.org/10.1126/science.2756425.
73. Buchberger A, Theyssen H, Schröder H, McCarty JS, Virgallita G, Milkereit P, Reinstein J, Bukau B. 1995. Nucleotide-induced conformational changes in the ATPase and substrate binding domains of the DnaK chaperone provide evidence for interdomain communication. J Biol Chem 270:16903–16910. https://doi.org/10.1074/jbc.270.28.16903.
74. Bukau B, Horwich AL. 1998. The Hsp70 and Hsp60 chaperone machines. Cell 92:351–366. https://doi.org/10.1016/s0092-8674(00)80928-9.
75. Liu Q, Hendrickson WA. 2007. Insights into Hsp70 chaperone activity from a crystal structure of the yeast Hsp110 Sse1. Cell 131:106–120. https://doi.org/10.1016/j.cell.2007.08.039.
76. Cheetham ME, Caplan AJ. 1998. Structure, function and evolution of DnaJ: conservation and adaptation of chaperone function. Cell Stress Chaperones 3:28–36.
77. Greene MK, Maskos K, Landry SJ. 1998. Role of the J-domain in the cooperation of Hsp40 with Hsp70. Proc Natl Acad Sci U S A 95:6108–6113. https://doi.org/10.1073/pnas.95.11.6108.
78. Jiang J, Maes EG, Taylor AB, Wang L, Hinck AP, Lafer EM, Sousa R. 2007. Structural basis of J cochaperone binding and regulation of Hsp70. Mol Cell 28:422–433. https://doi.org/10.1016/j.molcel.2007.08.022.
79. Suzuki K, Sako K, Akiyama K, Isoda M, Senoo C, Nakajo N, Sagata N. 2015. Identification of non-Ser/Thr-Pro consensus motifs for Cdk1 and their roles in mitotic regulation of C2H2 zinc finger proteins and Ect2. Sci Rep 5:7929. https://doi.org/10.1038/srep07929.
80. Kusubata M, Matsuoka Y, Tsujimura K, Ito H, Ando S, Kamijo M, Yasuda H, Ohba Y, Okumura E, Kishimoto T, Inagaki M. 1993. cdc2 kinase phosphorylation of desmin at three serine/threonine residues in the amino-terminal head domain. Biochem Biophys Res Commun 190:927–934. https://doi.org/10.1006/bbrc.1993.1138.
81. Satterwhite LL, Lohka MJ, Wilson KL, Scherson TY, Cisek LJ, Corden JL, Pollard TD. 1992. Phosphorylation of myosin-II regulatory light chain by cyclin-p34cdc2: a mechanism for the timing of cytokinesis. J Cell Biol 118:595–605. https://doi.org/10.1083/jcb.118.3.595.
82. Harvey SL, Charlet A, Haas W, Gygi SP, Kellogg DR. 2005. Cdk1-dependent regulation of the mitotic inhibitor Wee1. Cell 122:407–420. https://doi.org/10.1016/j.cell.2005.05.029.
83. Isoda M, Sako K, Suzuki K, Nishino K, Nakajo N, Ohe M, Ezaki T, Kanemori Y, Inoue D, Ueno H, Sagata N. 2011. Dynamic regulation of Emi2 by Emi2-bound Cdk1/Plk1/CK1 and PP2A-B56 in meiotic arrest of Xenopus eggs. Dev Cell 21:506–519. https://doi.org/10.1016/j.devcel.2011.06.029.
84. McCusker D, Denison C, Anderson S, Egelhofer TA, Yates JR, Gygi SP, Kellogg DR. 2007. Cdk1 coordinates cell-surface growth with the cell cycle. Nat Cell Biol 9:506–515. https://doi.org/10.1038/ncb1568.
85. Albanèse V, Yam A-W, Baughman J, Parnot C, Frydman J. 2006. Systems analyses reveal two chaperone networks with distinct functions in eukaryotic cells. Cell 124:75–88. https://doi.org/10.1016/j.cell.2005.11.039.
86. Boorstein WR, Ziegelhoffer T, Craig EA. 1994. Molecular evolution of the HSP70 multigene family. J Mol Evol 38:1–17. https://doi.org/10.1007/bf00175490.
87. Kim S, Schilke B, Craig EA, Horwich AL. 1998. Folding in vivo of a newly translated yeast cytosolic enzyme is mediated by the SSA class of cytosolic yeast Hsp70 proteins. Proc Natl Acad Sci U S A 95:12860–12865. https://doi.org/10.1073/pnas.95.22.12860.
88. Oka M, Nakai M, Endo T, Lim CR, Kimata Y, Kohno K. 1998. Loss of Hsp70-Hsp40 chaperone activity causes abnormal nuclear distribution and aberrant microtubule formation in M-phase of Saccharomyces cerevisiae. J Biol Chem 273:29727–29737. https://doi.org/10.1074/jbc.273.45.29727.
89. Shulga N, Roberts P, Gu Z, Spitz L, Tabb MM, Nomura M, Goldfarb DS. 1996. In vivo nuclear transport kinetics in Saccharomyces cerevisiae: a role for heat shock protein 70 during targeting and translocation. J Cell Biol 135:329–339. https://doi.org/10.1083/jcb.135.2.329.
90. Mayer MP, Bukau B. 1998. Hsp70 chaperone systems: diversity of cellular functions and mechanism of action. Biol Chem 379:261–268.
91. Stone DE, Craig EA. 1990. Self-regulation of 70-kilodalton heat shock proteins in Saccharomyces cerevisiae. Mol Cell Biol 10:1622–1632. https://doi.org/10.1128/mcb.10.4.1622.
92. Shorter J, Lindquist S. 2005. Prions as adaptive conduits of memory and inheritance. Nat Rev Genet 6:435–450. https://doi.org/10.1038/nrg1616.

93. Jones GW, Masison DC. 2003. Saccharomyces cerevisiae Hsp70 mutations affect [PSI+] prion propagation and cell growth differently and implicate Hsp40 and tetratricopeptide repeat cochaperones in impairment of [PSI+]. Genetics 163:495–506.
94. Killian AN, Hines JK. 2018. Chaperone functional specificity promotes yeast prion diversity. PLoS Pathog 14:e1006695. https://doi.org/10.1371/journal.ppat.1006695.
95. Higurashi T, Hines JK, Sahi C, Aron R, Craig EA. 2008. Specificity of the J-protein Sis1 in the propagation of 3 yeast prions. Proc Natl Acad Sci U S A 105:16596–16601. https://doi.org/10.1073/pnas.0808934105.
96. Tchounwou PB, Yedjou CG, Patlolla AK, Sutton DJ. 2012. Heavy metal toxicity and the environment, p 133–164. *In* Luch A (ed), Molecular, clinical and environmental toxicology. Springer, Basel, Switzerland.
97. Schirmer EC, Homann OR, Kowal AS, Lindquist S. 2004. Dominant gain-of-function mutations in Hsp104p reveal crucial roles for the middle region. Mol Biol Cell 15:2061–2072. https://doi.org/10.1091/mbc.e02-08-0502.
98. Lee J-H, Mand MR, Kao C-H, Zhou Y, Ryu SW, Richards AL, Coon JJ, Paull TT. 2018. ATM directs DNA damage responses and proteostasis via genetically separable pathways. Sci Signal 11:eaaan5598. https://doi.org/10.1126/scisignal.aan5598.